AD_____

AWARD NUMBER: W81XWH-08-1-0042

TITLE: PTEN Loss Antagonizes Calcitriol-Mediated Growth Inhibition in Prostate Epithelial Cells

PRINCIPAL INVESTIGATOR: Linara S. Axanova, M.S.

CONTRACTING ORGANIZATION: Wake Forest University Health Sciences
Winston-Salem, NC 27157

REPORT DATE: May 2009

TYPE OF REPORT: Annual Summary

PREPARED FOR: U.S. Army Medical Research and Materiel Command
Fort Detrick, Maryland 21702-5012

REPORT DOCUMENTATION PAGE

Form Approved
OMB No. 0704-0188

1. REPORT DATE	2. REPORT TYPE	3. DATES COVERED
1 May 2009	Annual Summary	21 Apr 2008 – 20 Apr 2009

4. TITLE AND SUBTITLE

PTEN Loss Antagonizes Calcitriol-Mediated Growth Inhibition in Prostate Epithelial Cells

5a. CONTRACT NUMBER

5b. GRANT NUMBER
W81XWH-08-1-0042

5c. PROGRAM ELEMENT NUMBER

6. AUTHOR(S)

Linara S. Axanova, M.S.

E-Mail: laxanova@wfubmc.edu

5d. PROJECT NUMBER

5e. TASK NUMBER

5f. WORK UNIT NUMBER

7. PERFORMING ORGANIZATION NAME(S) AND ADDRESS(ES)

Wake Forest University Health Sciences
Winston-Salem, NC 27157

8. PERFORMING ORGANIZATION REPORT NUMBER

9. SPONSORING / MONITORING AGENCY NAME(S) AND ADDRESS(ES)
U.S. Army Medical Research and Materiel Command
Fort Detrick, Maryland 21702-5012

10. SPONSOR/MONITOR'S ACRONYM(S)

11. SPONSOR/MONITOR'S REPORT NUMBER(S)

12. DISTRIBUTION / AVAILABILITY STATEMENT
Approved for Public Release; Distribution Unlimited

13. SUPPLEMENTARY NOTES

14. ABSTRACT
1-alpha, 25-dihydroxy vitamin D3 (1,25(OH)2D3) elicits antiproliferative effects in a variety of cancer cell types including prostate cells while the PI3K/AKT pathway stimulates pro-survival signals. The antiproliferative effect of 1,25(OH)2D3 almost universally involves upregulation of p21 and/or p27, while activation of PI3K/AKT downregulates p21 and p27 levels. We hypothesized that inhibition of the PI3K/AKT pathway synergizes with the antiproliferative signaling of 1,25(OH)2D3. We demonstrate that pharmacological inhibitors of PI3K or Akt restored sensitivity to antiproliferative effects of 1,25(OH)2D3 in 1,25(OH)2D3-insensitive cells and synergized to inhibit the growth of Pten-/- mouse prostatic epithelial cells, DU145, LNCaP and primary human prostate cancer cell strains. The inhibitors used included API-2 (Triciribine) and GSK690693 which are currently in clinical trials for treatment of cancer. The combination of 1,25(OH)2D3 and AKT inhibitor API-2 led to a cooperative increase in G1 arrest and in the induction of senescence. AKT is commonly activated by PTEN loss, therefore we evaluated the role of Pten in responsiveness to 1,25(OH)2D3 using shRNA knockdown and by in vitro knockout of Pten. We found that Pten status did not affect responsiveness to the antiproliferative action of 1,25(OH)2D3. These findings provide the rationale for the development of therapeutic interventions utilizing 1,25(OH)2D3 or its analogs combined with inhibition of PI3K/AKT for the treatment of prostate cancer.

15. SUBJECT TERMS
Vitamin D3, AKT inhibition, synergism, prostate cancer

16. SECURITY CLASSIFICATION OF:			17. LIMITATION OF ABSTRACT	18. NUMBER OF PAGES	19a. NAME OF RESPONSIBLE PERSON
a. REPORT	b. ABSTRACT	c. THIS PAGE			USAMRMC
U	U	U	UU	53	19b. TELEPHONE NUMBER *(include area code)*

Table of Contents

Introduction

Prostate cancer (CaP) is the most commonly diagnosed cancer and the second most common cause of cancer death in American men (1). It has been suggested that the development of clinical prostate cancer may be associated with vitamin D_3 deficiency (2, 3).

Vitamin D is a hormone that can be obtained from the diet or produced endogenously by a series of reactions that culminates in the most active metabolite of vitamin D, 1α, 25$(OH)_2$-vitamin D_3 (1,25$(OH)_2D_3$), also called calcitriol. 1,25$(OH)_2D_3$ elicits antiproliferative effects in a variety of cancer cell types including cell lines derived from prostate (4, 5). The ability of 1,25$(OH)_2D_3$ to inhibit prostate growth was also demonstrated in primary prostatic cells from histologically normal, benign prostatic hyperplasia, and prostate cancer specimens (6), in multiple prostate cancer cell lines (7-9), in xenograft models of prostate cancer (10, 11) as well as in Dunning rat prostate model (12). The anticancer mechanisms of 1,25$(OH)_2D_3$'s action include induction of cell cycle arrest, promotion of differentiation, inhibition of proliferation and angiogenesis, as well as inhibition of invasive and migratory potential of cancer cells [reviewed in (13)].

Classical actions of 1,25$(OH)_2D_3$ are mediated through the vitamin D receptor (VDR) which is a member of a superfamily of nuclear steroid hormone receptors. Upon 1,25$(OH)_2D_3$ binding VDR translocates to the nucleus, dimerizes with retinoid X receptor (RXR) and modulates the expression of target genes. Although a number of 1,25$(OH)_2D_3$ responsive genes are known, the exact mechanism of growth regulation by 1,25$(OH)_2D_3$ is not completely defined; however, an increase in p21 and/or p27 is an almost universal feature (4).

One of the central contributing factors which facilitates the survival of prostate cancer cells is attributed to the phosphoinositol-3 kinase PI3K-AKT pathway. Activated AKT phosphorylates a host of proteins that affect cell growth, cell cycle entry, and cell survival. The AKT pathway presents an attractive target for anticancer therapies and several AKT inhibitors have been developed that demonstrate anticancer activity in preclinical and clinical studies (14). In prostate cancer, activation of AKT occurs most frequently due to the loss of tumor suppressor phosphatase and a tensin homologue deleted in chromosome ten (PTEN)(15-17). Loss of PTEN protein occurs in 20% of primary prostate tumors and this loss is highly correlated with advanced tumor grade and stage with 50% of metastatic tumors exhibiting a loss of PTEN protein (18). Moreover, loss of heterozygosity (LOH) is found in 20% to 60% of metastatic tumors (19). Data suggests that advancing disease is associated with a progressive loss of PTEN or an accumulation of mutations in the PTEN gene. Loss of PTEN and activation of AKT has been shown to downregulate the expression of p21 and p27 by a number of mechanisms (20-25).

In our preliminary data we had shown that *Pten* WT mouse prostatic epithelial cells (MPEC) exhibit significant levels of growth-inhibition in response to the presence of 1,25$(OH)_2D_3$, whereas growth of *Pten*-/- MPECs in which Pten was lost *in vivo* are not affected by 1,25$(OH)_2D_3$. Pretreatment of *Pten*-/- MPECs with PI3K/AKT inhibitors resulted in the partial restoration of sensitivity to 1,25$(OH)_2D_3$. Given our preliminary findings and the existing data contained within recent literature, we proposed the hypothesis that **1,25$(OH)_2D_3$-mediated growth inhibition of prostate epithelial cells is antagonized by PTEN loss**.

Body

SOW TASK 1:

In our preliminary data we had shown that *Pten* WT mouse prostatic epithelial cells (MPEC) exhibit significant levels of growth-inhibition in response to the presence of $1,25(OH)_2D_3$, whereas growth of *Pten*-/- MPECs in which Pten was lost *in vivo* are not affected by $1,25(OH)_2D_3$. In SOW Task 1 we proposed to evaluate the role of Pten in $1,25(OH)_2D_3$-mediated growth inhibition in more controlled settings. Thus, we generated MPEC in which Pten expression was suppressed using an shRNA approach. MPEC WFU3 were infected with either lentivirus expressing scrambled shRNA or with lentivirus expressing shRNA targeting Pten (the details of the method is described in the Materials and Methods section of the attached manuscript). Single cell clones of each of the cell types were established and Pten status was verified by Immunoblot (Fig. S5A of the attached manuscript). WFU3 control MPEC clones and WFU3 MPEC clones with Pten knocked down to undetectable levels were treated with increasing doses of $1,25(OH)_2D_3$ as was proposed in SOW Task 1C. There was no significant difference in the response to $1,25(OH)_2D_3$ based on Pten status; both cell types remained $1,25(OH)_2D_3$-sensitive (Fig. 4B). This suggested that suppression of Pten expression by shRNA was not sufficient to abrogate the growth-inhibitory qualities of $1,25(OH)_2D_3$ in MPEC.

Since gene suppression using an shRNA approach has the potential disadvantages of incomplete suppression of target gene expression and also possible off-target effects, we sought to establish a cell line with acute *in vitro* deletion of Pten as was proposed in SOW Task 1A. Thus, we isolated $Pten^{lox/lox}$ MPEC from prostates of $Pten^{lox/lox}$ Cre-recombinase negative animals and infected them with lentivirus expressing self-deleting Cre-recombinase (for more details see Material and Methods section of the attached manuscript). PCR and Immunoblot analysis of the deletion demonstrated the absence of Pten expression in the cells infected with Cre-recombinase (Fig. S5B and S5C).

As proposed in SOW Task 1C the control $Pten^{lox/lox}$ MPEC and $Pten^{-/-}$ ($Pten^{lox/lox}$ infected with Cre-recombinase lentivirus) cells were treated with increasing concentrations of $1,25(OH)_2D_3$ and cell viability was evaluated by trypan blue exclusion assay as well as by clonogenic survival. We observed that *in vitro* accute loss if Pten did not significantly affect the ability of $1,25(OH)_2D_3$ to inhibit the growth of the cells (Fig. 4C). These results were confirmed by clonogenic assays (Fig. S6, S7). Together, these data demonstrate that while *in vivo* loss of Pten was associated with resistance to $1,25(OH)_2D_3$-mediated growth inhibition of MPEC, *in vitro* suppression or loss of Pten in MPECs was not associated with increased resistance to $1,25(OH)_2D_3$.

As our hypothesis that Pten status determines the ability of prostate cells to be growth inhibited by $1,25(OH)_2D_3$ was not confirmed we did not continue with SOW Task 1D which was intended to determine the role of lipid and protein phosphatase activity of Pten in $1,25(OH)_2D_3$-mediated growth inhibition. For the same reason we did not proceed with the SOW Task 1E which aimed to establish the role of PTEN loss in response of human prostate cancer cells to $1,25(OH)_2D_3$.

As it was mentioned above our preliminary pretreatment of *Pten*-/- MPECs with PI3K/AKT inhibitors resulted in the partial restoration of sensitivity to $1,25(OH)_2D_3$. In addition, activation of AKT has been shown to downregulate the expression of p21 and p27 by a number of mechanisms (20-25) while the antiproliferative effects of $1,25(OH)_2D_3$ involve upregulation of p21 and/or p27 (4), we next hypothesized that pharmacological inhibitors of AKT will cooperate with the antiproliferative actions of $1,25(OH)_2D_3$ in prostate cancer cells. These experiments were not proposed in Statement of Work submitted to DOD; however, have a straight relevance to the research project as well as high importance due to the fact that a number of AKT inhibitors as well as $1,25(OH)_2D_3$ or its analogs are currently in clinical trials for treatment of cancer. The potential existence of synergism between these compounds could significantly enhance the therapeutic efficacy of these clinically relevant drugs while reducing the potential side effects.

We first utilized a pharmacological inhibitor of PI3K/AKT, LY294002 (27). Cells were treated with increasing doses of $1,25(OH)_2D_3$ or LY294002 or with multiple combinations of the two compounds and the number of viable cells was assessed. Synergism was assessed with the Chou-Talalay method (28) in which the combination index (CI) values < 1 indicates presence of synergism.

We found that LNCaP cells, which lack functional PTEN, and are moderately sensitive to growth inhibition by $1,25(OH)_2D_3$, demonstrated statistically significant synergism between $1,25(OH)_2D_3$ and LY294002 (Fig. 1A, Table 1, and Fig S1A).

DU145 cells (wild-type PTEN) are known to be resistant to the antiproliferative effects of $1,25(OH)_2D_3$ (29). While 100 nM $1,25(OH)_2D_3$ did not inhibit growth of DU145 cells, pretreatment of DU145 cells with 5 μM LY294002 sensitized the cells to $1,25(OH)_2D_3$ treatment leading to a reduction in the number of viable cells to 40% compared to treatment with LY294002 alone (Fig 1B and S1B). We found significant synergism across multiple doses of both compounds (Table 1).

Next we tested for synergism between LY294002 and $1,25(OH)_2D_3$ in *Pten*$^{-/-}$ MPEC, which were isolated from 8-10 week old animals with targeted deletion of Pten in the prostate and are $1,25(OH)_2D_3$-insensitive. Pre-treatment of Pten$^{-/-}$ MPECs (clone 11) with LY294004 partially restored sensitivity to $1,25(OH)_2D_3$-mediated antiproliferative effects and synergized to inhibit the growth of the cells (Fig. 1C, Table 1, and Fig S1C).

These data demonstrated that LY294002 which is a potent inhibitor of both PI3K and AKT can synergize with $1,25(OH)_2D_3$ to inhibit prostate cancer cell proliferation. However, LY294002 has recently been reported to have many other off-target effects (30). Therefore, to validate synergism with AKT-inhibition specifically, we used two different AKT inhibitors which currently are in clinical trials for cancer treatment: API-2 (Triciribine), which selectively inhibits Akt1/2/3 without inhibiting PI3K or PDK (31) and GSK690693, an ATP competitive AKT inhibitor (32). We also expanded the effects to primary human prostate cancer epithelial cells.

The combination of $1,25(OH)_2D_3$ with API-2 elicited synergistic growth inhibition of DU145 cells as well as of human primary prostate cancer cell strains WFU275CA and WFU273CA (Table 2, Table S1, Fig 2A,B Fig S2A,B, and Fig S3). The combination of another AKT inhibitor GSK690693 with $1,25(OH)_2D_3$ also elicited strong to very strong synergistic growth inhibition of DU145 cells (Fig.2C, S2C and Table 2) and of human primary prostatic epithelial cells (Fig.2D and S2D). Together these data demonstrated that inhibition of the AKT pathway synergizes with $1,25(OH)_2D_3$ to inhibit the growth of prostate cancer cell.

Having demonstrated synergism between $1,25(OH)_2D_3$ and AKT inhibitors we sought to explore the mechanism. First, we performed video time-lapse microscopy analysis of DU145 cells treated with API-2 (0.25 μM) or $1,25(OH)_2D_3$ (100 nM) alone as well as in combination. We did not observe any considerable apoptosis in any of the treatments. Next we evaluated cell cycle distribution of DU145 cells treated with API-2 or $1,25(OH)_2D_3$. Cell cycle analysis demonstrated a small but statistically significant increase in G_1-arrested cells treated with the combination of API-2 at 0.25 μM with $1,25(OH)_2D_3$ at 10 nM compared to either agent alone (Fig. 3A).

Since we were unable to detect apoptosis and the effects on cell cycle, although significant, were modest, we next evaluated the effects of the combination on senescence. In the human primary cancer cell strain WFU273Ca $1,25(OH)_2D_3$ was able to induce SA-β-Gal activity which was associated with morphological features consistent with senescence (Fig 3B,C). Treatment with 100 nM $1,25(OH)_2D_3$ was able to induce senescence in 16.8% of the WFU273CA cells (Table S2). The combination of API-2 and $1,25(OH)_2D_3$ cooperated with each other at the higher doses tested to induce greater SA-β-Gal activity which was statistically significant by ANOVA (Fig 3B, 3C and Table S2).

DU145 cells also showed significant cooperativity for induction of SA-β-gal. Treatment with 0.25 μM API-2 induced senescence in 5.11% of DU145 cells and 100 nM $1,25(OH)_2D_3$ induced senescence in 2.64% of the cell; the combination of the two led to 10.48% of the cells to undergo senescence (Fig 3D) which was statistically significant by ANOVA. Representative photographs are shown in Fig. S4.

Together these data suggest that synergism between API-2 and $1,25(OH)_2D_3$ in prostate cancer cells might be a result of cooperative induction of cell cycle arrest and senescence.

SOW TASK 2 progress:

Currently we are performing experiments described in the SOW Task 2A which aims to determine downstream mediator of the AKT axis and $1,25(OH)_2D_3$ signaling that is involved in the synergism between AKT inhibitors and $1,25(OH)_2D_3$. Our main hypothesis is that p21 and p27 are the primary players involved in this interplay. Thus, we are evaluating the levels of expression of p21 and p27 protein in sub-cellular compartments of prostate cells upon treatment with $1,25(OH)_2D_3$ alone, AKT inhibitor alone or the combination of these two agent. We are utilizing Immunofluoresence microscopy methods as well as Immunoblotting of the cytoplasmic and nuclear fractions of the cells.

We are in the process of the establishing the shRNA vectors that will knock down p21 and p27 protein in order to evaluate the importance of these proteins in the cross talk between the AKT signaling and antiproliferative $1,25(OH)_2D_3$-signlaing (as described on the SOW Task 2B).

Key research accomplishments

- a manuscript in preparation for submission
- have generated the MPEC clones with Pten knocked down with shRNA as well as control clones (with confirmed stable knockdown by Immunoblott)
- have generated $Pten^{lox/lox}$ MPEC and $Pten^{-/-}$ ($Pten^{lox/lox}$ infected with Cre-recombinase lentivirus) cell lineages (with confirmed Pten deletion by PCR and Immunoblot)

Reportable outcomes

We have demonstrated that pharmacological inhibitors of PI3K or Akt restored sensitivity to antiproliferative effects of $1,25(OH)_2D_3$ in $1,25(OH)_2D_3$-insensitive cells and synergized to inhibit the growth of Pten-/- mouse prostatic epithelial cells, DU145, LNCaP and primary human prostate cancer cell strains. The inhibitors used included API-2 (Triciribine) and GSK690693 which are currently in clinical trials for treatment of cancer. The combination of $1,25(OH)_2D_3$ and AKT inhibitor API-2 led to a cooperative increase in G_1 arrest and in the induction of senescence. AKT is commonly activated by PTEN loss, therefore we evaluated the role of Pten in responsiveness to $1,25(OH)_2D_3$ using shRNA knockdown and by *in vitro* knockout of Pten. We found that Pten status did not affect responsiveness to the antiproliferative action of $1,25(OH)_2D_3$.

Conclusions

We found that Pten status *per ce* did not affect responsiveness to the antiproliferative action of $1,25(OH)_2D_3$. In addition, we discovered that pharmacological inhibitors of PI3K or AKT are capable of restoring sensitivity to antiproliferative effects of $1,25(OH)_2D_3$ in $1,25(OH)_2D_3$-insensitive cells. In addition, the PI3K/AKT inhibitors tested synergized to inhibit the growth of Pten-/- mouse prostatic epithelial cells, DU145, LNCaP and primary human prostate cancer cell strains. Inhibitors of the PI3K/AKT pathway included Triciribine and GSK690693 which are currently in clinical trials for treatment of cancer and the effect of the combination was 10 to 1000 times greater than the AKT inhibitor alone as was demonstrated by Dose Reduction Indexes. This synergistic effect has not been previously demonstrated and could significantly enhance the therapeutic efficacy of these clinically relevant drugs while reducing the potential side effects. Thus, these findings provide the rationale for the development of therapeutic interventions utilizing $1,25(OH)_2D_3$ or its analogs combined with inhibition of PI3K/AKT for the treatment of prostate cancer.

References:

1. Cancer Facts and Figures.: American Cancer Society, 2007.
2. Schwartz, G. G. and Hulka, B. S. Is vitamin D deficiency a risk factor for prostate cancer? (Hypothesis). Anticancer Res, *10:* 1307-1311, 1990.
3. Ahonen, M. H., Tenkanen, L., Teppo, L., Hakama, M., and Tuohimaa, P. Prostate cancer risk and prediagnostic serum 25-hydroxyvitamin D levels (Finland). Cancer Causes Control, *11:* 847-852, 2000.
4. Banerjee, P. and Chatterjee, M. Antiproliferative role of vitamin D and its analogs--a brief overview. Mol Cell Biochem, *253:* 247-254, 2003.
5. Rao, A., Woodruff, R. D., Wade, W. N., Kute, T. E., and Cramer, S. D. Genistein and vitamin D synergistically inhibit human prostatic epithelial cell growth. J Nutr, *132:* 3191-3194, 2002.
6. Peehl, D. M., Skowronski, R. J., Leung, G. K., Wong, S. T., Stamey, T. A., and Feldman, D. Antiproliferative effects of 1,25-dihydroxyvitamin D3 on primary cultures of human prostatic cells. Cancer Res, *54:* 805-810, 1994.
7. Skowronski, R. J., Peehl, D. M., and Feldman, D. Vitamin D and prostate cancer: 1,25 dihydroxyvitamin D3 receptors and actions in human prostate cancer cell lines. Endocrinology, *132:* 1952-1960, 1993.
8. Miller, G. J., Stapleton, G. E., Hedlund, T. E., and Moffat, K. A. Vitamin D receptor expression, 24-hydroxylase activity, and inhibition of growth by 1alpha,25-dihydroxyvitamin D3 in seven human prostatic carcinoma cell lines. Clin Cancer Res, *1:* 997-1003, 1995.
9. Zhao, X. Y., Peehl, D. M., Navone, N. M., and Feldman, D. 1alpha,25-dihydroxyvitamin D3 inhibits prostate cancer cell growth by androgen-dependent and androgen-independent mechanisms. Endocrinology, *141:* 2548-2556, 2000.
10. Blutt, S. E. and Weigel, N. L. Vitamin D and prostate cancer. Proc Soc Exp Biol Med, *221:* 89-98, 1999.
11. Ahmed, S., Johnson, C. S., Rueger, R. M., and Trump, D. L. Calcitriol (1,25-dihydroxycholecalciferol) potentiates activity of mitoxantrone/dexamethasone in an androgen independent prostate cancer model. J Urol, *168:* 756-761, 2002.
12. Getzenberg, R. H., Light, B. W., Lapco, P. E., Konety, B. R., Nangia, A. K., Acierno, J. S., Dhir, R., Shurin, Z., Day, R. S., Trump, D. L., and Johnson, C. S. Vitamin D inhibition of prostate adenocarcinoma growth and metastasis in the Dunning rat prostate model system. Urology, *50:* 999-1006, 1997.
13. Krishnan, A. V., Peehl, D. M., and Feldman, D. Inhibition of prostate cancer growth by vitamin D: Regulation of target gene expression. J Cell Biochem, *88:* 363-371, 2003.
14. Cheng, G. Z., Park, S., Shu, S., He, L., Kong, W., Zhang, W., Yuan, Z., Wang, L. H., and Cheng, J. Q. Advances of AKT pathway in human oncogenesis and as a target for anti-cancer drug discovery. Curr Cancer Drug Targets, *8:* 2-6, 2008.
15. Li, D. M. and Sun, H. PTEN/MMAC1/TEP1 suppresses the tumorigenicity and induces G1 cell cycle arrest in human glioblastoma cells. Proc Natl Acad Sci U S A, *95:* 15406-15411, 1998.
16. Li, L., Ittmann, M. M., Ayala, G., Tsai, M. J., Amato, R. J., Wheeler, T. M., Miles, B. J., Kadmon, D., and Thompson, T. C. The emerging role of the PI3-K-Akt pathway in prostate cancer progression. Prostate Cancer Prostatic Dis, *8:* 108-118, 2005.
17. Rubin, M. A., Gerstein, A., Reid, K., Bostwick, D. G., Cheng, L., Parsons, R., and Papadopoulos, N. 10q23.3 loss of heterozygosity is higher in lymph node-positive (pT2-3,N+) versus lymph node-negative (pT2-3,N0) prostate cancer. Hum Pathol, *31:* 504-508, 2000.
18. Sansal, I. and Sellers, W. R. The biology and clinical relevance of the PTEN tumor suppressor pathway. J Clin Oncol, *22:* 2954-2963, 2004.
19. Sellers, W. and Sawyers, C. L. Somatic genetics of prostate cancer, oncogenes and tumor suppressors. *In:* P. W. Kantoff, P. R. Carroll, and A. V. D'Amico (eds.), Prostate Cancer: Principles and Practice. Philadelphia, PA: Lippencott, William & Wilkins, 2002.

20. Viglietto, G., Motti, M. L., Bruni, P., Melillo, R. M., D'Alessio, A., Califano, D., Vinci, F., Chiappetta, G., Tsichlis, P., Bellacosa, A., Fusco, A., and Santoro, M. Cytoplasmic relocalization and inhibition of the cyclin-dependent kinase inhibitor p27(Kip1) by PKB/Akt-mediated phosphorylation in breast cancer. Nat Med, *8:* 1136-1144, 2002.
21. Kops, G. J., de Ruiter, N. D., De Vries-Smits, A. M., Powell, D. R., Bos, J. L., and Burgering, B. M. Direct control of the Forkhead transcription factor AFX by protein kinase B. Nature, *398:* 630-634, 1999.
22. Mamillapalli, R., Gavrilova, N., Mihaylova, V. T., Tsvetkov, L. M., Wu, H., Zhang, H., and Sun, H. PTEN regulates the ubiquitin-dependent degradation of the CDK inhibitor p27(KIP1) through the ubiquitin E3 ligase SCF(SKP2). Curr Biol, *11:* 263-267, 2001.
23. Andreu, E. J., Lledo, E., Poch, E., Ivorra, C., Albero, M. P., Martinez-Climent, J. A., Montiel-Duarte, C., Rifon, J., Perez-Calvo, J., Arbona, C., Prosper, F., and Perez-Roger, I. BCR-ABL induces the expression of Skp2 through the PI3K pathway to promote p27Kip1 degradation and proliferation of chronic myelogenous leukemia cells. Cancer Res, *65:* 3264-3272, 2005.
24. Motti, M. L., Califano, D., Troncone, G., De Marco, C., Migliaccio, I., Palmieri, E., Pezzullo, L., Palombini, L., Fusco, A., and Viglietto, G. Complex regulation of the cyclin-dependent kinase inhibitor p27kip1 in thyroid cancer cells by the PI3K/AKT pathway: regulation of p27kip1 expression and localization. Am J Pathol, *166:* 737-749, 2005.
25. Zhou, B. P. and Hung, M. C. Novel targets of Akt, p21(Cipl/WAF1), and MDM2. Semin Oncol, *29:* 62-70, 2002.
26. Pfeifer, A., Brandon, E. P., Kootstra, N., Gage, F. H., and Verma, I. M. Delivery of the Cre recombinase by a self-deleting lentiviral vector: efficient gene targeting in vivo. Proc Natl Acad Sci U S A, *98:* 11450-11455, 2001.
27. Vlahos, C. J., Matter, W. F., Hui, K. Y., and Brown, R. F. A specific inhibitor of phosphatidylinositol 3-kinase, 2-(4-morpholinyl)-8-phenyl-4H-1-benzopyran-4-one (LY294002). J Biol Chem, *269:* 5241-5248, 1994.
28. Chou, T. C. and Talalay, P. Quantitative analysis of dose-effect relationships: the combined effects of multiple drugs or enzyme inhibitors. Adv Enzyme Regul, *22:* 27-55, 1984.
29. Zhuang, S. H., Schwartz, G. G., Cameron, D., and Burnstein, K. L. Vitamin D receptor content and transcriptional activity do not fully predict antiproliferative effects of vitamin D in human prostate cancer cell lines. Mol Cell Endocrinol, *126:* 83-90, 1997.
30. Ihle, N. T. and Powis, G. Take your PIK: phosphatidylinositol 3-kinase inhibitors race through the clinic and toward cancer therapy. Mol Cancer Ther, *8:* 1-9, 2009.
31. Yang, L., Dan, H. C., Sun, M., Liu, Q., Sun, X. M., Feldman, R. I., Hamilton, A. D., Polokoff, M., Nicosia, S. V., Herlyn, M., Sebti, S. M., and Cheng, J. Q. Akt/protein kinase B signaling inhibitor-2, a selective small molecule inhibitor of Akt signaling with antitumor activity in cancer cells overexpressing Akt. Cancer Res, *64:* 4394-4399, 2004.
32. Rhodes, N., Heerding, D. A., Duckett, D. R., Eberwein, D. J., Knick, V. B., Lansing, T. J., McConnell, R. T., Gilmer, T. M., Zhang, S. Y., Robell, K., Kahana, J. A., Geske, R. S., Kleymenova, E. V., Choudhry, A. E., Lai, Z., Leber, J. D., Minthorn, E. A., Strum, S. L., Wood, E. R., Huang, P. S., Copeland, R. A., and Kumar, R. Characterization of an Akt kinase inhibitor with potent pharmacodynamic and antitumor activity. Cancer Res, *68:* 2366-2374, 2008.

1,25-dihydroxyvitamin D_3 and PI3K/AKT inhibitors synergistically inhibit growth and cooperatively induce cell cycle arrest and senescence in prostate cancer cells

Linara S. Axanova[1], Yong Q. Chen[1], Thomas McCoy[2], Guangchao Sui[1] and Scott D. Cramer[1, 2].

[1]*Cancer Biology and* [2]*Public Health Science Departments, Wake Forest University School of Medicine, Winston Salem, NC.*

Correspondence: Scott D. Cramer, Department of Cancer Biology, Wake Forest University School of Medicine, Medical Center Blvd. Winston-Salem, NC 27157. Phone: (336) 713-7651, FAX (336) 713-7661, E-Mail scramer@wfubmc.edu

Running Title: Vitamin D_3 and AKT in prostate

Key Words: Vitamin D_3, AKT, prostate, cancer, synergism

Grant support: R01 CA101023 (NCI, NIH), PC073325 (DOD), RO1 CA106742-01A1

Statement of Translational Relevance

The presented manuscript demonstrates that various pharmacological inhibitors of the PI3K/AKT pathway (including Triciribine and GSK690693 which are currently in clinical trials for treatment of cancer) synergized with 1-alpha, 25-dihydroxy vitamin D_3 ($1,25(OH)_2D_3$) to inhibit the growth of prostate cancer cells. This effect was demonstrated in multiple prostate cancer cell types and strains. The effect of the combination was 10 to 1000 times greater than the AKT inhibitor alone as was demonstrated by Dose Reduction Indexes. This synergistic effect has not been previously demonstrated and could significantly enhance the therapeutic efficacy of these clinically relevant drugs while reducing the potential side effects.

Abstract: Purpose:1-alpha, 25-dihydroxy vitamin D3 (1,25(OH)2D3) inhibits proliferation in multiple cancer cell types including prostate cells and upregulates p21 and/or p27, while loss of Pten and PI3K/AKT activation stimulates survival and downregulates p21 and p27. We hypothesized that inhibition of the PI3K/AKT pathway synergizes with the antiproliferative signaling of 1,25(OH)2D3. Experimental Design: Viability, cell cycle distribution and senescence of cells were evaluated upon combinational treatment with $1,25(OH)_2D_3$ and pharmacological PI3K/AKT inhibitors. Pten was knockdown by shRNA or knockout by Cre-recombinase and responsiveness to $1,25(OH)_2D_3$ was evaluated. Results: Pharmacological inhibitors of PI3K or Akt restored sensitivity to antiproliferative effects of $1,25(OH)_2D_3$ in $1,25(OH)_2D_3$-insensitive cells and synergized to inhibit the growth of Pten-/- mouse prostatic epithelial cells, DU145, LNCaP and primary human prostate cancer cell strains. The inhibitors used included API-2 (Triciribine) and GSK690693 which are currently in clinical trials for treatment of cancer. The combination of $1,25(OH)_2D_3$ and AKT inhibitor API-2 led to a cooperative increase in G_1 arrest and in the induction of senescence. As AKT is commonly activated by PTEN loss, we evaluated the role of Pten in responsiveness to $1,25(OH)_2D_3$. We found that Pten knockdown or knockout did not reduce responsiveness to $1,25(OH)_2D_3$.

Conclusions: These findings provide the rationale for the development of therapeutic interventions utilizing $1,25(OH)_2D_3$ or its analogs combined with inhibition of PI3K/AKT for the treatment of prostate cancer.

Introduction

Prostate cancer (CaP) is the most commonly diagnosed cancer and the second most common cause of cancer death in American men (1). It has been suggested that the development of clinical prostate cancer may be associated with vitamin D_3 deficiency (2, 3). Vitamin D is a hormone that can be obtained from the diet or produced endogenously by a series of reactions that culminates in the most active metabolite of vitamin D, 1α, 25$(OH)_2$-vitamin D_3 (1,25$(OH)_2D_3$). 1,25$(OH)_2D_3$ elicits antiproliferative effects in a variety of cancer cell types including cell lines derived from prostate (4, 5). The ability of 1,25$(OH)_2D_3$ to inhibit prostate growth was also demonstrated in primary prostatic cells from histologically normal, benign prostatic hyperplasia, and prostate cancer specimens (6), in multiple prostate cancer cell lines (7-9), in xenograft models of prostate cancer (10, 11) as well as in Dunning rat prostate model (12). The anticancer mechanisms of 1,25$(OH)_2D_3$'s action include induction of cell cycle arrest, promotion of differentiation, inhibition of proliferation and angiogenesis, as well as inhibition of invasive and migratory potential of cancer cells [reviewed in (13)].

Classical actions of 1,25$(OH)_2D_3$ are mediated through the vitamin D receptor (VDR) which is a member of a superfamily of nuclear steroid hormone receptors. Upon 1,25$(OH)_2D_3$ binding VDR translocates to the nucleus, dimerizes with retinoid X receptor (RXR) and modulates the expression of target genes. Although a number of 1,25$(OH)_2D_3$ responsive genes are known, the exact mechanism of growth regulation by 1,25$(OH)_2D_3$ is not completely defined; however, an increase in p21 and/or p27 is an almost universal feature (4).

One of the central contributing factors which facilitates the survival of prostate cancer cells is attributed to the phosphoinositol-3 kinase PI3K-AKT pathway. Activated AKT phosphorylates a host of proteins that affect cell growth, cell cycle entry, and cell survival. The AKT pathway

presents an attractive target for anticancer therapies and several AKT inhibitors have been developed that demonstrate anticancer activity in preclinical and clinical studies (14). In prostate cancer, activation of AKT occurs most frequently due to the loss of tumor suppressor phosphatase and a tensin homologue deleted in chromosome ten (PTEN)(15-17). Loss of PTEN protein occurs in 20% of primary prostate tumors and this loss is highly correlated with advanced tumor grade and stage with 50% of metastatic tumors exhibiting a loss of PTEN protein (18). Moreover, loss of heterozygosity (LOH) is found in 20% to 60% of metastatic tumors (19). Data suggests that advancing disease is associated with a progressive loss of PTEN or an accumulation of mutations in the PTEN gene. Loss of PTEN and activation of AKT has been shown to downregulate the expression of p21 and p27 by a number of mechanisms (20-25). Since the antiproliferative effects of $1,25(OH)_2D_3$ involve upregulation of p21 and/or p27 (4) while activation of PI3K/AKT downregulates their expression (25), we hypothesized that pharmacological inhibitors of AKT will cooperate with the antiproliferative actions of $1,25(OH)_2D_3$ in prostate cancer cells.

Our results demonstrate that inhibition of PI3K or AKT synergized with $1,25(OH)_2D_3$ to inhibit the growth of human prostate cancer cell lines, primary human prostate cancer strains, and mouse prostatic epithelial cells (MPEC) and led to cooperative induction of G_1 arrest and senescence. Responsiveness to the antiproliferative effects of $1,25(OH)_2D_3$ was not dependent on Pten status. These findings provide the rationale for prostate cancer therapies involving use of AKT inhibitors and $1,25(OH)_2D_3$ in adjunctive therapy.

Materials and Methods

Materials. $1,25(OH)_2D_3$ (Biomol, Plymouth Meeting, PA) was reconstituted in 100% ethanol and stored at -80ºC. LY294002 (Sigma-Aldrich Co., St Louis, MO), GSK690693 (26) (a generous gift from GlaxoSmithKline, Collegeville, PA) and API-2 (27) (Calbiochem, La Jolla, CA) were reconstituted in DMSO and stored at -20ºC.

MPEC with *in vivo* deletion of Pten: $Pten^{-/-}$ MPEC were isolated from anterior prostates of 8-10 week old $Pten^{lox/lox}$ mice expressing Cre recombinase under the control of a modified rat prostate-specific probasin promoter (pbCre) (28). MPECs wild type for Pten were isolated from anterior prostates of 8-10 week old $Pten^{wt/lox;\ pbCre^-}$ mice. The method of isolation was developed in our laboratory and is previously described (29). MPEC were clonally selected using serial dilution as described (30) and Pten status was confirmed by PCR and Immunoblot (See Supplemental Methods).

MPECs with *in vitro* deletion of Pten: Pten lox/lox anterior MPECs were isolated from 8 week old $Pten^{lox/lox;\ pbCre^-}$ animals as described (29) and infected with self-deleting Cre-recombinase lentivirus (31). Deletion was validated by PCR and immunoblot (See Supplental Methods).

Tissue culture. LNCaP and DU145 cells (both from American Type Culture Collection, Manassas, VA) were grown in RPMI-1640 supplemented with 10% FBS and 1% Penicillin-Streptomycin. MPEC were grown as described previously (29). Two separate human prostate epithelial cancer cell strains were obtained from separate patients (labeled WFU273Ca and WFU275Ca), validated for histological origin, and maintained as previously described (32).

shRNA Infection. WFU3 MPEC (29) were infected with lentivirus expressing shRNA targeting Pten (gaa cct gat cat tat aga tat t) or control shRNA (gggc cat ggc acg tac ggc aag). Lentivirus production and infection procedure were previously described (33). MPECs were clonally selected using serial dilution and Pten status was confirmed by Immunoblot.

Growth assays for synergism determination. Cells were plated at 10^4 cells per 35 mm dish in triplicate. To determine synergism cells were treated with increasing doses of AKT inhibitor, increasing doses of $1,25(OH)_2D_3$ or multiple combinations of AKT inhibitor and $1,25(OH)_2D_3$. Briefly, 48 hr after plating the cell growth medium was replaced with 1 ml of experimental medium containing twice (2x) the indicated concentration of a PI3K/AKT inhibitor or vehicle (DMSO, 1x = 0.1% V/V). One hour later 1 ml of medium containing twice the final concentration of $1,25(OH)_2D_3$ or vehicle (ethanol, 1x = 0.1% V/V) was added to each dish. DU145, LNCaP and $Pten^{-/-}$ MPEC remained in the experimental medium until the controls reached 80-90% confluence. For WFU273Ca and WFU275Ca and for all experiments using GSK690693 the experimental medium was replaced every 48hr. Viable cells were counted with a hemacytometer after trypan blue exclusion. Results of representative experiments are shown.

Flow cytometry: Flow cytometry was performed as described (5) using Becton Dickinson FACSCaliber and analyzed by the Cell Quest Pro v.6.0 program (Becton Dickinson, Mansfiled, MA). Data were processed with ModFit LT v.2.0 software (Verity Software House, Topsham, MN). Each treatment was performed in triplicate and the experiment was conducted three times.

Senescence-associated (SA)-β-galactosidase (gal) activity: Cells were cultured and treated as described above. After 5-7 days of treatment (SA)-β-galactosidase activity was evaluated by the method of Dimri et al. (34). Digital images were taken from 10 random areas at 20X magnification. Digital images were evaluated in Photoshop CS2 9.0.2 (Adobe Systems, San

Jose, CA). The number of SA-β-gal positive cells was counted in each image and presented as percent of total cell number ± SE.

Statistical Analyses: Synergism was assessed with CalcuSyn software (Biosoft, Ferguson, MO) as previously described (5). Briefly, the dose effect for each drug alone was determined based on the experimental observations using the median effect principle: the combination index (CI) for each combination was calculated according to the following equation: $CI = [(D)_1/(D_x)_1] + [(D)_2/(D_x)_2] + [(D)_1(D)_2/(D_x)_1(D_x)_2]$, where $(D)_1$ and $(D)_2$ are the doses of drug that have *x* effect when used in combination and $(D_x)_1$ and $(D_x)_2$ are the doses of drug 1 and drug 2 that have the same *x* effect when used alone. CI = 1 represents the conservation isobologram and indicates additive effects. CI values < 1 indicate a more than expected additive effect (synergism).
All other statistical analyses were performed using the statistical software package NCSS 2002 (Number Cruncher Statistical Systems, Kaysville, UT). Differences in growth data were determined by two-way ANOVA controlling for $1,25(OH)_2D_3$ or PI3K/AKT inhibitor dose with post hoc analysis by Fisher's test. Cell cycle distribution and senescence analyses were performed using two-way ANOVA with post hoc analysis by Fisher's LSD test. In all cases, $P<0.05$ was considered significant.

Results

$1,25(OH)_2D_3$ and PI3K/Akt inhibitors synergistically inhibit prostate cancer cell growth.

To test whether inhibition of the PI3K/Akt pathway synergizes with $1,25(OH)_2D_3$ treatment to inhibit the growth of prostatic cells we first utilized a pharmacological inhibitor of PI3K/AKT, LY294002 (35). Cells were treated with increasing doses of $1,25(OH)_2D_3$ or LY294002 or with multiple combinations of the two compounds and the number of viable cells was assessed. Synergism was assessed with the Chou-Talalay method (36) in which the combination index (CI) values < 1 indicates presence of synergism.

We found that LNCaP cells, which lack functional PTEN and are moderately sensitive to growth inhibition by $1,25(OH)_2D_3$, demonstrated statistically significant synergism between $1,25(OH)_2D_3$ and LY294002 at lower doses of $1,25(OH)_2D_3$ (Fig. 1A, Table 1, and Fig S1A). The combination of 1 nM $1,25(OH)_2D_3$ treatment with 0.2 μM, 1 μM or 5 μM LY294002 demonstrated statistically significant synergism as determined by CI values from isobologram analysis (Table 1). The dose-reduction index (DRI) for each of the drugs is also depicted in Table 1 and presents a measure of how much the dose of each drug in a synergistic combination may be reduced at a given effect level compared with the doses of each drug alone (36).

DU145 cells (wild-type PTEN) are known to be resistant to the antiproliferative effects of $1,25(OH)_2D_3$ (37). Consistent with this, we found that $1,25(OH)_2D_3$ did not significantly affect growth of DU145 cells (Fig 1B and S1B). While 100 nM $1,25(OH)_2D_3$ did not inhibit growth of DU145 cells, pretreatment of DU145 cells with 5 μM LY294002 sensitized the cells to $1,25(OH)_2D_3$ treatment leading to a reduction in the number of viable cells to 40% compared to treatment with LY294002 alone (Fig 1B and S1B). We found significant synergism across multiple doses of both compounds (Table 1).

Next we tested for synergism between LY294002 and 1,25$(OH)_2D_3$ in *Pten*$^{-/-}$ MPEC, which were isolated from 8-10 week old animals with targeted deletion of Pten in the prostate and are 1,25$(OH)_2D_3$-insensitive. Pre-treatment of Pten$^{-/-}$ MPECs (clone 11) with LY294004 partially restored sensitivity to 1,25$(OH)_2D_3$-mediated antiproliferative effects and synergized to inhibit the growth of the cells (Fig. 1C, Table 1, and Fig S1C).

These data demonstrated that LY294002 which is a potent inhibitor of both PI3K and AKT can synergize with 1,25$(OH)_2D_3$ to inhibit prostate cancer cell proliferation. However, LY294002 has recently been reported to have many other off-target effects (38). Therefore, to validate synergism with AKT-inhibition specifically, we used two different AKT inhibitors which currently are in clinical trials for cancer treatment: API-2 (Triciribine), which selectively inhibits Akt1/2/3 without inhibiting PI3K or PDK (27) and GSK690693, an ATP competitive AKT inhibitor (26). We also expanded the effects to primary human prostate cancer epithelial cells.

The combination of 1,25$(OH)_2D_3$ with API-2 elicited synergistic growth inhibition of DU145 cells as well as of human primary prostate cancer cell strains WFU275CA and WFU273CA (Table 2, Table S1, Fig 2A,B Fig S2A,B, and Fig S3). DU145 cells treated with the combination of API-2 and 1,25$(OH)_2D_3$ demonstrated strong synergism at all doses tested as determined by CI values from isolobolgrams (Table 2). Note that the treatment with API-2 and 1,25$(OH)_2D_3$ was applied only once after which the cells were allowed to grow until the cells in either of the treatment groups were 90% confluent.

The combination of API-2 and 1,25$(OH)_2D_3$ used for treatment of primary epithelial prostate cancer cell strain WFU275Ca demonstrated statistically significant moderate to strong synergism (Table 2) with DRI values as high as 283.0 for 1,25$(OH)_2D_3$ and 9.6 for API-2. Similar results were observed in WFU273Ca (Fig.S3A and Table S1).

The combination of another AKT inhibitor GSK690693 with $1,25(OH)_2D_3$ also elicited strong to very strong synergistic growth inhibition of DU145 cells (Fig.2C, S2C and Table 2). DRI values for GSK690693 ranged from 3.5 to 214.4 for GSK690693. DRI is calculated using the equation: $(DRI)_1=(D_x)_1/D_1$ and $(DRI)_2=(D_x)_2/D_2$, where $(D)_1$ and $(D)_2$ are the doses of drug that have *x* effect when used in combination and $(D_x)_1$ and $(D_x)_2$ are the doses of drug 1 and drug 2 that have the same *x* effect when used alone. DRI values for treatment of DU145 with $1,25(OH)_2D_3$ are extremely high as the x effect of the $1,25(OH)_2D_3$ alone was near zero.

Treatment of cells with and $1,25(OH)_2D_3$ were applied every 48hr because single treatment with GSK690693 and $1,25(OH)_2D_3$ did not render a synergistic effect (data not shown). We also tested the combination of GSK690693 with $1,25(OH)_2D_3$ in human primary prostatic epithelial cells (Fig.2D and S2D) which elicited strong synergism and DRI values as high as 5158.7 for $1,25(OH)_2D_3$ and as high as 51.7 for GSK690693 (Table 2).

Together these data support our hypothesis that inhibition of the AKT pathway synergizes with $1,25(OH)_2D_3$ to inhibit the growth of prostate cancer cell.

$1,25(OH)_2D_3$ and PI3K/Akt inhibitors cooperate to inhibit cell cycle progression and induce senescence

Having demonstrated synergism between $1,25(OH)_2D_3$ and AKT inhibitors we sought to explore the mechanism. First, we performed video time-lapse microscopy analysis of DU145 cells treated with API-2 (0.25 μM) or $1,25(OH)_2D_3$ (100 nM) alone as well as in combination. We did not observe any considerable apoptosis in any of the treatments (data not shown). Next we evaluated cell cycle distribution of DU145 cells treated with API-2 or $1,25(OH)_2D_3$. Cell cycle analysis demonstrated a small but statistically significant increase in G_1-arrested cells treated

with the combination of API-2 at 0.25 μM with 1,25$(OH)_2D_3$ at 10 nM compared to either agent alone (Fig. 3A).

Since we were unable to detect apoptosis and the effects on cell cycle, although significant, were modest, we next evaluated the effects of the combination on senescence. In the human primary cancer cell strain WFU273Ca 1,25$(OH)_2D_3$ was able to induce SA-β-Gal activity which was associated with morphological features consistent with senescence (Fig 3B,C). Treatment with 100 nM 1,25$(OH)_2D_3$ was able to induce senescence in 16.8% of the WFU273CA cells (Table S2). The combination of API-2 and 1,25$(OH)_2D_3$ cooperated with each other at the higher doses tested to induce greater SA-β-Gal activity which was statistically significant by ANOVA (Fig 3B, 3C and Table S2). Interestingly, inhibition of the AKT pathway with API-2 alone induced senescence in WFU273Ca cells with 0.5μM API-2 causing 30% of the cells to undergo senescence, suggesting a role of the AKT pathway in the prevention of senescence in these cells (Table S2).

DU145 cells also showed significant cooperativity for induction of SA-β-gal. Treatment with 0.25 μM API-2 induced senescence in 5.11% of DU145 cells and 100 nM 1,25$(OH)_2D_3$ induced senescence in 2.64% of the cell; the combination of the two led to 10.48% of the cells to undergo senescence (Fig 3D) which was statistically significant by ANOVA. Representative photographs are shown in Fig. S4.

Together these data suggest that synergism between API-2 and 1,25$(OH)_2D_3$ in prostate cancer cells might be a result of cooperative induction of cell cycle arrest and senescence.

The role of Pten status in sensitivity to antiproliferative action of 1,25$(OH)_2D_3$.

Activation of AKT in prostate cancer occurs most frequently due to the loss of the tumor suppressor phosphatase and a tensin homologue deleted in chromosome ten (PTEN), which is

found in 20% of primary tumors and more than 50% of metastatic tumors (18)**.** Thus, we wanted to evaluate the role of Pten in the antiproliferative signaling of $1,25(OH)_2D_3$. To test this we used $Pten^{+/+}$ MPEC and *Pten* $^{-/-}$ MPEC which were isolated from $Pten^{wt/lox;\ pbCre^-}$ and from $Pten^{lox/lox;\ pbCre+}$ animals, respectively. Animals were 8-10 weeks old and while $Pten^{wt/lox;\ pbCre^-}$ prostates did not show any abnormalities. $Pten^{-/-}$ prostates were presented with tumors consistent with other reports for this strain (39). Both types of MPEC were clonally selected using serial dilution as described (30) and Pten status was confirmed by PCR and Immunoblot (not shown).

$Pten^{+/+}$ and $Pten^{-/-}$ MPEC clones were treated with increasing doses of $1,25(OH)_2D_3$ and while $Pten^{+/+}$ clones showed a dose-dependent growth inhibition, the same concentrations of $1,25(OH)_2D_3$ did not inhibit growth of $Pten^{-/-}$ clones and in some clones marginally stimulated growth (Fig. 4A). This suggested that Pten loss might desensitize MPEC to the growth inhibitory effects of $1,25(OH)_2D_3$; alternatively, other events associated with tumorigenesis resulting from Pten loss may be responsible for the observed insensitivity to $1,25(OH)_2D_3$ antiproliferative action. Noteworthy, this resistance to the antiproliferative effects of $1,25(OH)_2D_3$ in $Pten^{-/-}$ MPEC was overcome by LY294002 treatment (Fig. 1C).

In order to evaluate the role of Pten in $1,25(OH)_2D_3$-mediated growth inhibition in more controlled settings we generated MPEC in which Pten expression was suppressed using an shRNA approach. MPEC WFU3 (29) were infected with either lentivirus expressing scrambled shRNA or with lentivirus expressing shRNA targeting Pten. Single cell clones of each of the cell types were established and Pten status was verified by Immunoblot (Fig. S5A). WFU3 control MPEC clones and WFU3 MPEC clones with Pten knocked down to undetectable levels were treated with increasing doses of $1,25(OH)_2D_3$. There was no significant difference in the response to $1,25(OH)_2D_3$ based on Pten status; both cell types remained $1,25(OH)_2D_3$-sensitive

(Fig. 4B). This suggested that suppression of Pten expression *per ce* is not sufficient to abrogate the growth-inhibitory qualities of $1,25(OH)_2D_3$ in MPEC.

Since gene suppression using an shRNA approach has the potential disadvantages of incomplete suppression of target gene expression and also possible off-target effects, we sought to establish a cell line with acute *in vitro* deletion of Pten. Thus, we isolated $Pten^{lox/lox}$ MPEC from prostates of $Pten^{lox/lox}$ Cre-recombinase negative animals and infected them with lentivirus expressing self-deleting Cre-recombinase (31). PCR and Immunoblot analysis of the deletion demonstrated the absence of Pten expression in the cells infected with Cre-recombinase (Fig. S5B and S5C).

The control $Pten^{lox/lox}$ MPEC and $Pten^{-/-}$ ($Pten^{lox/lox}$ infected with Cre-recombinase lentivirus) cells were treated with increasing concentrations of $1,25(OH)_2D_3$. We observed that *in vitro* loss if Pten did not significantly affect the ability of $1,25(OH)_2D_3$ to inhibit the growth of the cells (Fig. 4C). These results were confirmed by clonogenic assays (Fig. S6, S7). Together, these data demonstrate that while *in vivo* loss of Pten was associated with resistance to $1,25(OH)_2D_3$-mediated growth inhibition of MPEC, *in vitro* suppression or loss of Pten in MPECs was not associated with increased resistance to $1,25(OH)_2D_3$.

Discussion

In this study we showed that AKT inhibitors in combination with $1,25(OH)_2D_3$ synergistically inhibit the growth of prostate cancer cells. The effect was observed with multiple inhibitors of PI3K and/or AKT and in multiple cell lines as well as primary human prostate cancer samples. Interestingly both cells that were wild-type for Pten and cells that lacked Pten were sensitive to the synergistic effects observed, suggesting broad applicability to prostate cancer.

Mechanistically, we observed moderate effects on cell cycle progression and larger effects on the induction of senescence. No evidence of apoptosis was identified. These studies are important because the two AKT inhibitors that we used, API-2 (Triciribine) and GSK690693, have entered Phase I and II clinical trials for various cancers (14, 26, 40), and therefore the results could have clinical translation relatively rapidly. However, a factor complicating the use of AKT inhibitors is that the AKT pathway presents one of the most important pathways for normal cell survival. It is not clear yet whether treatment with AKT inhibitors will demonstrate acceptable levels of toxicity at doses that are therapeutically effective. Our data using $1,25(OH)_2D_3$ in combination with the AKT inhibitors that show DRIs for the AKT drugs that range from 10 to over 1000, suggest that more therapeutic efficacy can be achieved by potentially less systemically toxic levels of the drugs.

$1,25(OH)_2D_3$ used as a single agent has been shown to possess anticancer qualities in a number of cancer models but has toxicities associated with calcium mobilization at doses that are therapeutically effective. One strategy to overcome this problem is the creation of less calcemic $1,25(OH)_2D_3$ analogs. Another strategy is to organize the treatment regimen in a way that allows reduction of side-effects; for instance, weekly oral high-dose $1,25(OH)_2D_3$ administration is well-tolerated in androgen independent prostate cancer patients (41). Another strategy is to combine $1,25(OH)_2D_3$ with other agents to develop therapeutic interventions that allow dose reduction, and thus alleviation of toxicities, while maintaining the growth inhibitory potential. Clinical trials utilizing $1,25(OH)_2D_3$ or its analogs in combination with chemotherapy in advanced prostate cancer have demonstrated the feasibility of the use of $1,25(OH)_2D_3$ for treatment of advanced prostate cancer (41-43). Beer et al. reported an 81% response rate for the combination of $1,25(OH)_2D_3$ and docetaxel in metastatic prostate cancer versus an expected response of 40% to 50% for docetaxel alone (41). The DRIs for $1,25(OH)_2D_3$ in combination

with AKT inhibitors, suggest that this combination could achieve therapeutic efficacy at non-toxic levels of $1,25(OH)_2D_3$.

We investigated the mechanistic basis for the observed synergism and found that it was largely attributable to enhanced senescence. Interestingly, overexpression of activated AKT itself can lead to oncogene-induced senescence, which must be overcome for the development of invasive carcinoma. Expression of activated AKT-1 in the mouse ventral prostate (*AKT1*-tg mouse) leads to prostatic intraepithelial noeplasia (PIN), which by itself fails to progress to invasive carcinoma (44). These PIN lesions were shown to exhibit enhanced senescence with associated increased p27 expression (44). Human PIN lesions were also positive for increased senescence that was associated with higher p27 levels. The authors hypothesized that overexpression of activated AKT leads to senescence in a p27 dependent manner and this prevents the development of invasive carcinoma. To test this they crossed the *AKT1*-tg mouse with mice containing targeted disruption of p27 (44). Loss of a single copy of the p27 gene led to invasive carcinoma. These data indicate that critical levels of p27 expression are needed to act as an important brake on the promotion of invasive carcinoma by activation of the AKT pathway. The results suggest that agents that enhance p27 expression may be beneficial therapeutic agents for prostate cancer. $1,25(OH)_2D_3$ increases the steady-state levels of p27 protein in prostate cancer cells (45) and our data show that it induces senescence in prostate cancer cells. These data suggest that $1,25(OH)_2D_3$, or one of its analogs, should be explored for their ability to block progression of PIN lesions to invasive carcinoma.

In summary, $1,25(OH)_2D_3$ and AKT inhibitors synergistically inhibit prostate cancer growth through induction of senescence. These data have implications for the clinical use of these agents in prostate cancer patients and may be important for progression in high-risk patients.

Acknowledgement

We are grateful to GlaxoSmithKline (Collegeville, PA) which generously provided GSK690693 used in the study. We thank Dr.George Kulik (Department of Cancer Biology, Wake Forest University School of Medicine) for providing us with API-2 and SH-5.

Table 1) Synergism between $1,25(OH)_2D_3$ and LY294002***

	$1,25(OH)_2D_3$, nM	LY294002, μM	CI*	DRI**		Synergism
				$1,25(OH)_2D_3$	LY294002	
LNCaP						
	1	0.2	0.171	8.2	20.7	Strong
	1	1	0.298	10.9	4.8	Strong
	1	0.5	0.675	26.3	1.6	Moderate
DU145						
	1	2.5	0.408	513.8	2.5	Intermediate
	1	5	0.650	666.0	1.5	Intermediate
	10	2.5	0.382	58.2	2.8	Intermediate
	10	5	0.654	67.7	1.6	Intermediate
	10	10	0.801	117.6	1.3	Moderate
	100	2.5	0.489	6.4	3.0	Intermediate
	100	5	0.585	9.5	2.1	Intermediate
	100	10	0.701	14.9	1.6	Intermediate
Pten-/- MPEC						
	10	10	0.220	$4.9*10^4$	4.6	Strong
	100	10	0.133	8969.7	7.5	Strong

*Combination Index (CI<0.1 indicates Very Strong Synergism; 0.1÷0.3 Strong Synergism; 0.3÷0.7 Synergism; 0.70÷0.85 Moderate Synergism; 0.85÷0.90 Slight Synergism; 0.90÷1.10 Nearly Additive Synergism)

**Dose Response Index

*** Data are from assays depicted in Figure S1A, only statistically significantly different means by ANOVA are depicted.

Table 2) Synergism between $1,25(OH)_2D_3$ and AKT Inhibitors***

	1,25(OH)2D3, nM	AKT inhibitor, nM	CI*	DRI**		Synergism
				$1,25(OH)_2D_3$	AKT inhibitor	
DU145						
AKT Inhibitor: API-2						
	0.1	50	$0.18*10^{-6}$	$5.5*10^{4}$	$4.0*10^{6}$	Very Strong
	0.1	100	$0.12*10^{-6}$	$8.7*10^{4}$	$4.4*10^{6}$	Very Strong
	0.1	500	$7.98*10^{-6}$	$1.3*10^{5}$	$1.9*10^{6}$	Very Strong
	0.1	1000	$9.82*10^{-6}$	$1.2*10^{5}$	$7.4*10^{5}$	Very Strong
	1	50	$0.75*10^{-6}$	$1.3*10^{4}$	$1.8*10^{7}$	Very Strong
	1	100	$0.55*10^{-6}$	$1.8*10^{4}$	$1.6*10^{7}$	Very Strong
	1	500	$0.60*10^{-b}$	$1.7*10^{a}$	$2.7*10^{b}$	Very Strong
	1	1000	$0.54*10^{-6}$	$1.9*10^{4}$	$1.6*10^{6}$	Very Strong
	10	50	0.001	872,1	$8.8*10^{6}$	Very Strong
	10	100	0.001	1014.8	$5.7*10^{6}$	Very Strong
	10	500	0.001	1950.4	$3.5*10^{6}$	Very Strong
	10	1000	0.001	1461.5	$1.1*10^{6}$	Very Strong
	100	50	0.007	135.6	$1.9*10^{7}$	Very Strong
	100	100	0.005	206.7	$1.9*10^{7}$	Very Strong
	100	500	0.006	180.3	$3.1*10^{6}$	Very Strong
	100	1000	0.005	193.0	$1.7*10^{6}$	Very Strong
WFU275CA						
AKT inhibitor: API-2						
	0.1	0.1	0.799	283.0	1.3	Moderate
	1	0.05	0.720	12.2	1.6	Moderate
	1	0.1	0.714	36.9	1.5	Moderate
	10	0.025	0.216	9.0	9.6	Strong
	10	0.05	0.169	22.5	8.0	Strong
	10	0.1	0.176	52.0	6.4	Strong
DU145						
AKT inhibitor: GSK690693						
	10	1	0.003	$1.1*10^{b}$	391.3	Very Strong
	10	10	0.070	$6.5*10^{4}$	14.3	Very Strong
	100	0.1	0.0001	$2.3*10^{4}$	2241.4	Very Strong
	100	1	0.004	$3.9*10^{4}$	268.7	Very Strong
	100	10	0.010	$1.5*10^{6}$	96.9	Very Strong
	100	100	0.061	$6.6*10^{6}$	16.3	Very Strong
	100	1000	0.281	$6.0*10^{7}$	3.5	Strong
WFU273CA						
AKT inhibitor: GSK690693						
	0.1	1000	0.7730	5158.7	1.3	Moderate
	1	10	0.062	37.1	28.5	Very Strong
	1	100	0.120	255.9	8.7	Strong
	1	1000	0.747	550.1	1.3	Moderate
	10	10	0.115	10.5	51.7	Strong
	10	100	0.234	14.1	6.1	Strong
	10	1000	0.344	215.4	3.0	Intermediate

*Combination Index (CI<0.1 indicates Very Strong Synergism; 0.1÷0.3 Strong Synergism; 0.3÷0.7 Synergism; 0.70÷0.85 Moderate Synergism; 0.85÷0.90 Slight Synergism; 0.90÷1.10 Nearly Additive Synergism)

**Dose Response Index. DRI is calculated using the equation: $(DRI)_1=(D_x)_1/D_1$ and $(DRI)_2=(D_x)_2/D_2$, where $(D)_1$ and $(D)_2$ are the doses of drug that have *x* effect when used in combination and $(D_x)_1$ and $(D_x)_2$ are the doses of drug 1 and drug 2 that have the same *x* effect when used alone. DRI values for $1,25(OH)_2D_3$ treatment in DU145 are high due to inability of the program to correctly calculate DRI based on the formula as the x effect of the $1,25(OH)_2D_3$ alone is near zero.

*** Data are from assays depicted in Figure S2 and S3, only statistically significantly different means by ANOVA are depicted.

Figure 1

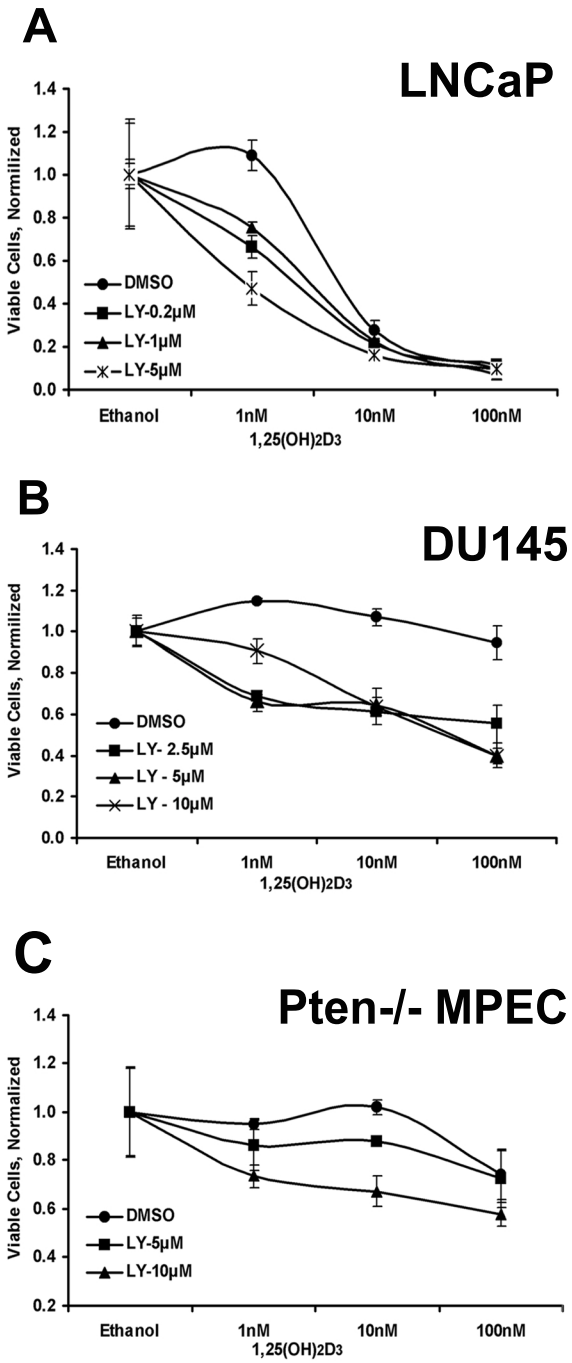
A
LNCaP
Viable Cells, Normilized
1.4
1.2
1.0
0.8
0.6
0.4
0.2
0.0
DMSO
LY-0.2μM
LY-1μM
LY-5μM
Ethanol
1nM
10nM
100nM
1,25(OH)2D3
B
DU145
Viable Cells, Normilized
DMSO
LY- 2.5μM
LY - 5μM
LY - 10μM
Ethanol
1nM
10nM
100nM
1,25(OH)2D3
C
Pten-/- MPEC
Viable Cells, Normalized
1.4
1.2
1.0
0.8
0.6
0.4
0.2
DMSO
LY-5μM
LY-10μM
Ethanol
1nM
10nM
100nM
1,25(OH)2D3

Figure 2

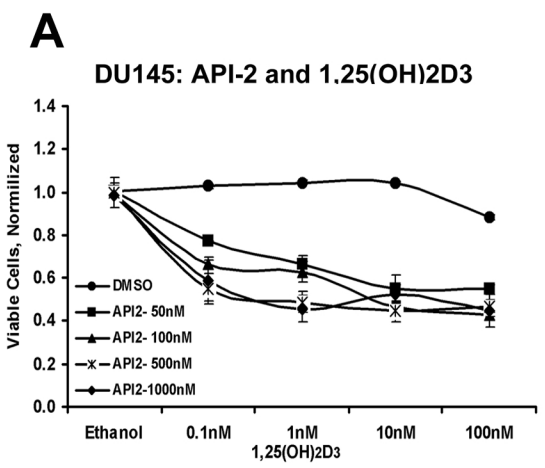
A
DU145: API-2 and 1.25(OH)2D3
Viable Cells, Normilized
1.4
1.2
1.0
0.8
0.6
0.4
0.2
0.0
DMSO
API2- 50nM
API2- 100nM
API2- 500nM
API2-1000nM
Ethanol
0.1nM
1nM
10nM
100nM
1,25(OH)2D3

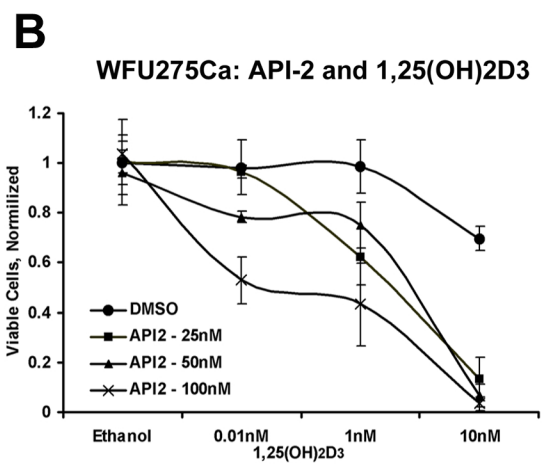
B
WFU275Ca: API-2 and 1,25(OH)2D3
Viable Cells, Normilized
1.2
1
0.8
0.6
0.4
0.2
0
DMSO
API2 - 25nM
API2 - 50nM
API2 - 100nM
Ethanol
0.01nM
1nM
10nM
1,25(OH)2D3

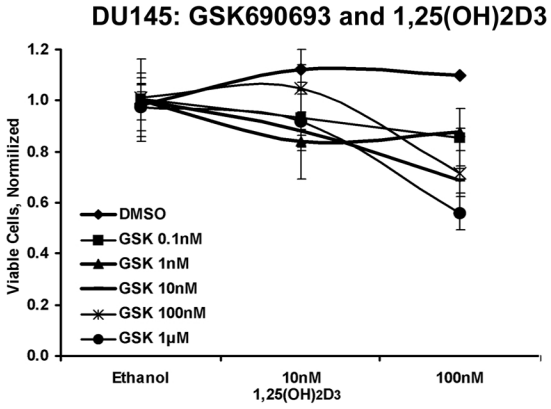
C
DU145: GSK690693 and 1,25(OH)2D3
Viable Cells, Normilized
1.2
1.0
0.8
0.6
0.4
0.2
0.0
DMSO
GSK 0.1nM
GSK 1nM
GSK 10nM
GSK 100nM
GSK 1µM
Ethanol
10nM
100nM
1,25(OH)2D3

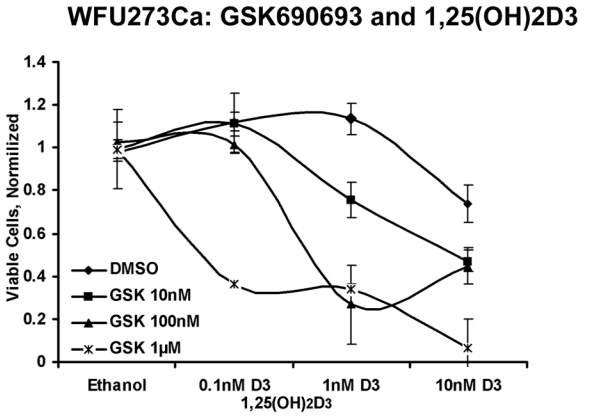
D
WFU273Ca: GSK690693 and 1,25(OH)2D3
Viable Cells, Normilized
1.4
1.2
1
0.8
0.6
0.4
0.2
0
DMSO
GSK 10nM
GSK 100nM
GSK 1µM
Ethanol
0.1nM D3
1nM D3
10nM D3
1,25(OH)2D3

Figure 3

A

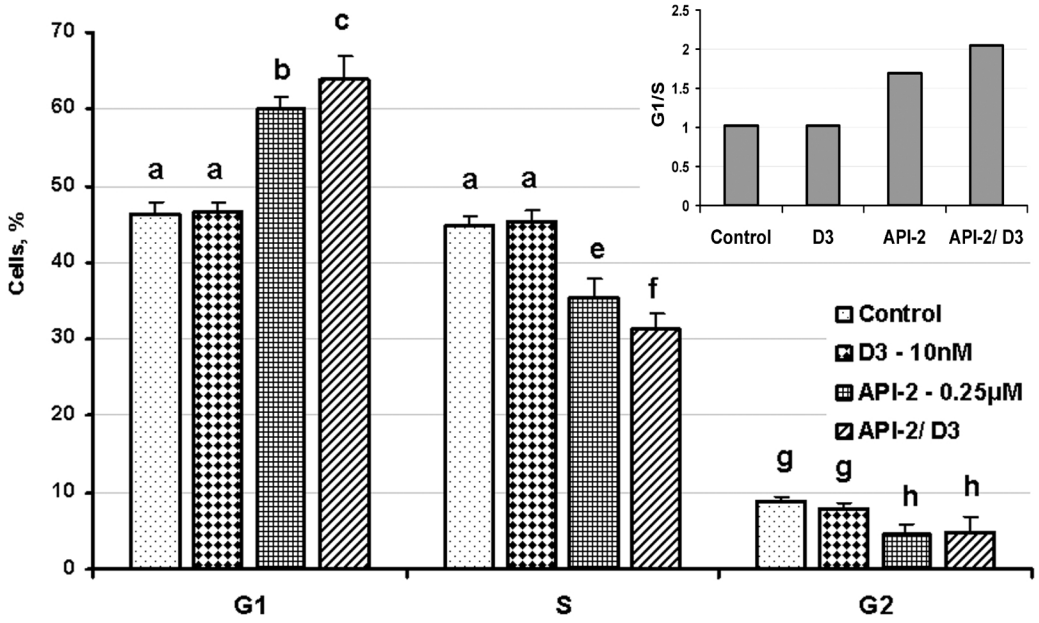

B

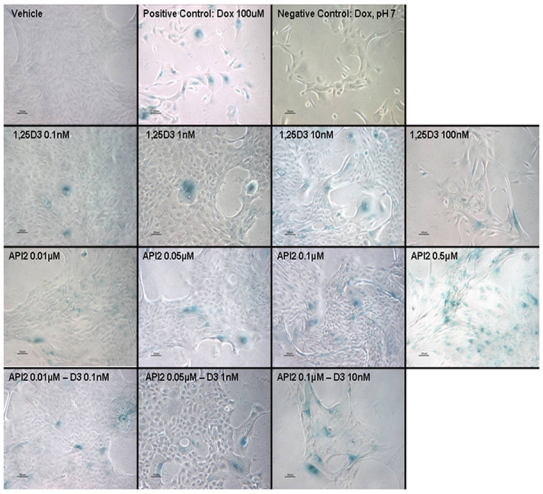

C

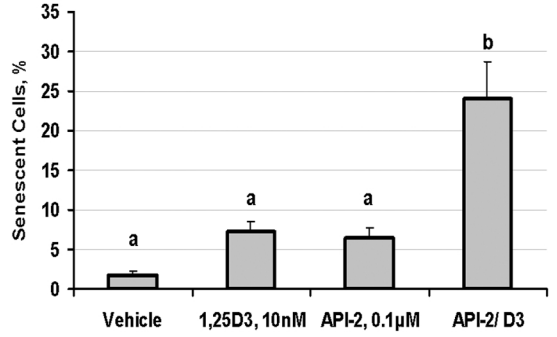

D

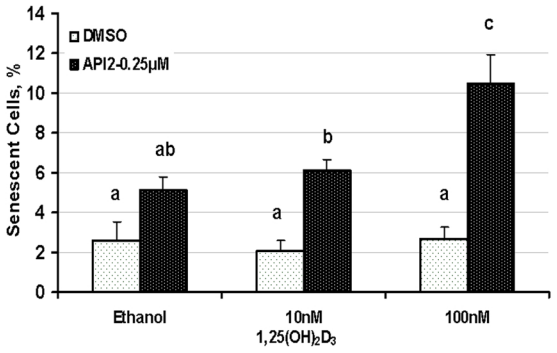

Figure 4

A

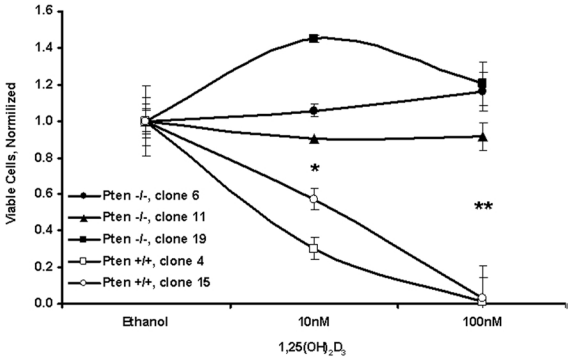
Viable Cells, Normilized
1.6
1.4
1.2
1.0
0.8
0.6
0.4
0.2
0.0
Pten -/-, clone 6
Pten -/-, clone 11
Pten -/-, clone 19
Pten +/+, clone 4
Pten +/+, clone 15
*
**
Ethanol
10nM
100nM
1,25(OH)2D3

B

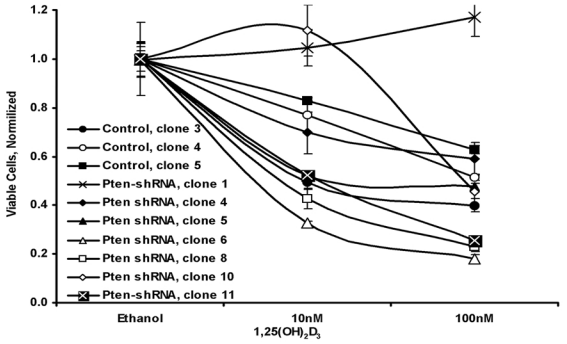
Viable Cells, Normilized
1.2
1.0
0.8
0.6
0.4
0.2
0.0
Control, clone 3
Control, clone 4
Control, clone 5
Pten-shRNA, clone 1
Pten shRNA, clone 4
Pten shRNA, clone 5
Pten shRNA, clone 6
Pten shRNA, clone 8
Pten shRNA, clone 10
Pten-shRNA, clone 11
Ethanol
10nM
100nM
1,25(OH)2D3

C

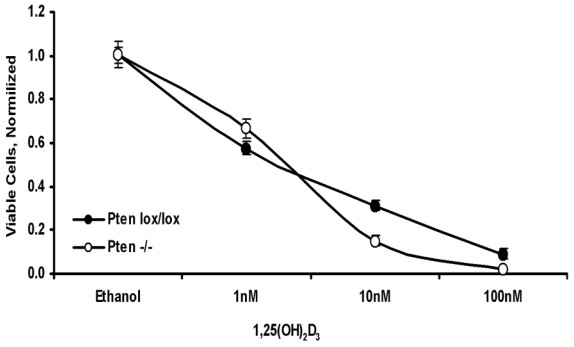
Viable Cells, Normilized
1.2
1.0
0.8
0.6
0.4
0.2
0.0
Pten lox/lox
Pten -/-
Ethanol
1nM
10nM
100nM
1,25(OH)2D3

Figure Legends

Figure 1. LY294002 and 1,25(OH)$_2$D$_3$ synergistically inhibits growth of LNCaP, DU145 and Pten-/- MPEC. Growth inhibition of LNCaP(**A**), DU145(**B**) and Pten-/- MPEC (in vivo deletion of Pten) (**C**) in response to LY294002 and 1,25(OH)$_2$D$_3$ alone or in combination. Cells were grown, treated and analyzed as described in Materials and Methods. Each point represents the mean and standard deviation of triplicate plates after normalization of cell number to controls (0.1% ethanol).

Figure 2. AKT inhibitors API-2 and GSK690693 synergize with 1,25(OH)$_2$D$_3$ to inhibit growth of DU145 cells and human primary prostate cancer strains.. Growth inhibition of DU145 cells (**A**) and human primary cancer cell strain WFU275CA (**B**) in response to API-2 and 1,25(OH)$_2$D$_3$ alone or in combination. Growth inhibition of DU145 cells (**C**) and human primary cancer cell strain WFU273CA (**D**) in response to GSK690693 and 1,25(OH)$_2$D$_3$ alone or in combination. Cells were grown, treated and analyzed as described in Materials and Methods.

Figure 3. AKT inhibitor API-2 and 1,25(OH)$_2$D$_3$ cooperate to induce G1-arrest and senescence. (A) 1,25(OH)$_2$D$_3$ and API-2 induce G1 arrest in cooperative manner in DU145 cells. DU145 cells were treated with the indicated doses for 24 hr and evaluated for cell cycle distribution as described in the Materials and Methods section. Insert demonstrates the G1/S ratios. Values are means for the triplicates ± SD. Means without a common letter are significantly different by ANOVA ($P < 0.05$). **(B)** 1,25(OH)$_2$D$_3$ and API-2 induce (SA)-β-galactosidase activity in a cooperative manner in WFU273CA cells**. (C)** Quantitative data from multiple images of WFU273Ca cells treated as indicated. Analysis was performed as described in the Materials and Methods section**.** Means ± SE are shown. Means without a common letter are significantly different by ANOVA ($P < 0.05$). **(D)** Quantitative data from ten images of DU145

cells treated as indicated. Analysis was performed as described in the Materials and Methods section**.** Means ± SE are shown. Means without a common letter are significantly different by ANOVA ($P < 0.05$). Representative photographs are shown in Fig S4. Cells were grown, treated and (SA)-β-galactosidase activity was evaluated as described in Materials and Methods.

Figure 4. *In Vivo* loss of Pten is associated with loss of sensitivity to $1,25(OH)_2D_3$ in MPECs while *in vitro* suppression or loss of Pten is not sufficient to antagonize $1,25(OH)_2D_3$-mediated growth suppression.

(A) Growth inhibition of $Pten^{+/+}$ and $Pten^{-/-}$ MPECs (*in vivo* loss of Pten) in response to $1,25(OH)_2D_3$. Means for the triplicates ± SD of a representative experiment are demonstrated. Interaction between Pten status and $1,25(OH)_2D_3$ dose was analyzed by two-way ANOVA (p=.003). * p=0.004; ** p<0.001. **(B)** Growth inhibition of WFU3 MPECs infected with Pten shRNA or scrambled shRNA in response to $1,25(OH)_2D_3$. Values are means for the triplicates ±SD. No statistically different response to $1,25(OH)_2D_3$ based on Pten status was observed. **(C)** Growth inhibition of $Pten^{lox/lox}$ and $Pten^{-/-}$ MPECs in response to $1,25(OH)_2D_3$. $Pten^{lox/lox}$ MPECs isolated from prostates of $Pten^{lox/lox}$ Cre-recombinase negative animals and infected with lentivirus expressing self-deleting Cre-recombinase to generate $Pten^{-/-}$ MPEC. Values are means for the triplicates ±SD. No statistically different response to $1,25(OH)_2D_3$ based on genetic background was observed.

References

1. Cancer Facts and Figures.: American Cancer Society, 2007.
2. Schwartz, G. G. and Hulka, B. S. Is vitamin D deficiency a risk factor for prostate cancer? (Hypothesis). Anticancer Res, *10:* 1307-1311, 1990.
3. Ahonen, M. H., Tenkanen, L., Teppo, L., Hakama, M., and Tuohimaa, P. Prostate cancer risk and prediagnostic serum 25-hydroxyvitamin D levels (Finland). Cancer Causes Control, *11:* 847-852, 2000.
4. Banerjee, P. and Chatterjee, M. Antiproliferative role of vitamin D and its analogs--a brief overview. Mol Cell Biochem, *253:* 247-254, 2003.
5. Rao, A., Woodruff, R. D., Wade, W. N., Kute, T. E., and Cramer, S. D. Genistein and vitamin D synergistically inhibit human prostatic epithelial cell growth. J Nutr, *132:* 3191-3194, 2002.
6. Peehl, D. M., Skowronski, R. J., Leung, G. K., Wong, S. T., Stamey, T. A., and Feldman, D. Antiproliferative effects of 1,25-dihydroxyvitamin D3 on primary cultures of human prostatic cells. Cancer Res, *54:* 805-810, 1994.
7. Skowronski, R. J., Peehl, D. M., and Feldman, D. Vitamin D and prostate cancer: 1,25 dihydroxyvitamin D3 receptors and actions in human prostate cancer cell lines. Endocrinology, *132:* 1952-1960, 1993.
8. Miller, G. J., Stapleton, G. E., Hedlund, T. E., and Moffat, K. A. Vitamin D receptor expression, 24-hydroxylase activity, and inhibition of growth by 1alpha,25-dihydroxyvitamin D3 in seven human prostatic carcinoma cell lines. Clin Cancer Res, *1:* 997-1003, 1995.
9. Zhao, X. Y., Peehl, D. M., Navone, N. M., and Feldman, D. 1alpha,25-dihydroxyvitamin D3 inhibits prostate cancer cell growth by androgen-dependent and androgen-independent mechanisms. Endocrinology, *141:* 2548-2556, 2000.
10. Blutt, S. E. and Weigel, N. L. Vitamin D and prostate cancer. Proc Soc Exp Biol Med, *221:* 89-98, 1999.
11. Ahmed, S., Johnson, C. S., Rueger, R. M., and Trump, D. L. Calcitriol (1,25-dihydroxycholecalciferol) potentiates activity of mitoxantrone/dexamethasone in an androgen independent prostate cancer model. J Urol, *168:* 756-761, 2002.
12. Getzenberg, R. H., Light, B. W., Lapco, P. E., Konety, B. R., Nangia, A. K., Acierno, J. S., Dhir, R., Shurin, Z., Day, R. S., Trump, D. L., and Johnson, C. S. Vitamin D inhibition of prostate adenocarcinoma growth and metastasis in the Dunning rat prostate model system. Urology, *50:* 999-1006, 1997.
13. Krishnan, A. V., Peehl, D. M., and Feldman, D. Inhibition of prostate cancer growth by vitamin D: Regulation of target gene expression. J Cell Biochem, *88:* 363-371, 2003.
14. Cheng, G. Z., Park, S., Shu, S., He, L., Kong, W., Zhang, W., Yuan, Z., Wang, L. H., and Cheng, J. Q. Advances of AKT pathway in human oncogenesis and as a target for anti-cancer drug discovery. Curr Cancer Drug Targets, *8:* 2-6, 2008.
15. Li, D. M. and Sun, H. PTEN/MMAC1/TEP1 suppresses the tumorigenicity and induces G1 cell cycle arrest in human glioblastoma cells. Proc Natl Acad Sci U S A, *95:* 15406-15411, 1998.
16. Li, L., Ittmann, M. M., Ayala, G., Tsai, M. J., Amato, R. J., Wheeler, T. M., Miles, B. J., Kadmon, D., and Thompson, T. C. The emerging role of the PI3-K-Akt pathway in prostate cancer progression. Prostate Cancer Prostatic Dis, *8:* 108-118, 2005.

17. Rubin, M. A., Gerstein, A., Reid, K., Bostwick, D. G., Cheng, L., Parsons, R., and Papadopoulos, N. 10q23.3 loss of heterozygosity is higher in lymph node-positive (pT2-3,N+) versus lymph node-negative (pT2-3,N0) prostate cancer. Hum Pathol, *31:* 504-508, 2000.
18. Sansal, I. and Sellers, W. R. The biology and clinical relevance of the PTEN tumor suppressor pathway. J Clin Oncol, *22:* 2954-2963, 2004.
19. Sellers, W. and Sawyers, C. L. Somatic genetics of prostate cancer, oncogenes and tumor suppressors. *In:* P. W. Kantoff, P. R. Carroll, and A. V. D'Amico (eds.), Prostate Cancer: Principles and Practice. Philadelphia, PA: Lippencott, William & Wilkins, 2002.
20. Viglietto, G., Motti, M. L., Bruni, P., Melillo, R. M., D'Alessio, A., Califano, D., Vinci, F., Chiappetta, G., Tsichlis, P., Bellacosa, A., Fusco, A., and Santoro, M. Cytoplasmic relocalization and inhibition of the cyclin-dependent kinase inhibitor p27(Kip1) by PKB/Akt-mediated phosphorylation in breast cancer. Nat Med, *8:* 1136-1144, 2002.
21. Kops, G. J., de Ruiter, N. D., De Vries-Smits, A. M., Powell, D. R., Bos, J. L., and Burgering, B. M. Direct control of the Forkhead transcription factor AFX by protein kinase B. Nature, *398:* 630-634, 1999.
22. Mamillapalli, R., Gavrilova, N., Mihaylova, V. T., Tsvetkov, L. M., Wu, H., Zhang, H., and Sun, H. PTEN regulates the ubiquitin-dependent degradation of the CDK inhibitor p27(KIP1) through the ubiquitin E3 ligase SCF(SKP2). Curr Biol, *11:* 263-267, 2001.
23. Andreu, E. J., Lledo, E., Poch, E., Ivorra, C., Albero, M. P., Martinez-Climent, J. A., Montiel-Duarte, C., Rifon, J., Perez-Calvo, J., Arbona, C., Prosper, F., and Perez-Roger, I. BCR-ABL induces the expression of Skp2 through the PI3K pathway to promote p27Kip1 degradation and proliferation of chronic myelogenous leukemia cells. Cancer Res, *65:* 3264-3272, 2005.
24. Motti, M. L., Califano, D., Troncone, G., De Marco, C., Migliaccio, I., Palmieri, E., Pezzullo, L., Palombini, L., Fusco, A., and Viglietto, G. Complex regulation of the cyclin-dependent kinase inhibitor p27kip1 in thyroid cancer cells by the PI3K/AKT pathway: regulation of p27kip1 expression and localization. Am J Pathol, *166:* 737-749, 2005.
25. Zhou, B. P. and Hung, M. C. Novel targets of Akt, p21(Cipl/WAF1), and MDM2. Semin Oncol, *29:* 62-70, 2002.
26. Rhodes, N., Heerding, D. A., Duckett, D. R., Eberwein, D. J., Knick, V. B., Lansing, T. J., McConnell, R. T., Gilmer, T. M., Zhang, S. Y., Robell, K., Kahana, J. A., Geske, R. S., Kleymenova, E. V., Choudhry, A. E., Lai, Z., Leber, J. D., Minthorn, E. A., Strum, S. L., Wood, E. R., Huang, P. S., Copeland, R. A., and Kumar, R. Characterization of an Akt kinase inhibitor with potent pharmacodynamic and antitumor activity. Cancer Res, *68:* 2366-2374, 2008.
27. Yang, L., Dan, H. C., Sun, M., Liu, Q., Sun, X. M., Feldman, R. I., Hamilton, A. D., Polokoff, M., Nicosia, S. V., Herlyn, M., Sebti, S. M., and Cheng, J. Q. Akt/protein kinase B signaling inhibitor-2, a selective small molecule inhibitor of Akt signaling with antitumor activity in cancer cells overexpressing Akt. Cancer Res, *64:* 4394-4399, 2004.

28. Wu, X., Wu, J., Huang, J., Powell, W. C., Zhang, J., Matusik, R. J., Sangiorgi, F. O., Maxson, R. E., Sucov, H. M., and Roy-Burman, P. Generation of a prostate epithelial cell-specific Cre transgenic mouse model for tissue-specific gene ablation. Mech Dev, *101:* 61-69, 2001.
29. Barclay, W. W. and Cramer, S. D. Culture of mouse prostatic epithelial cells from genetically engineered mice. Prostate, *63:* 291-298, 2005.
30. Barclay, W. W., Axanova, L. S., Chen, W., Romero, L., Maund, S. L., Soker, S., Lees, C. J., and Cramer, S. D. Characterization of adult prostatic progenitor/stem cells exhibiting self-renewal and multilineage differentiation. Stem Cells, *26:* 600-610, 2008.
31. Pfeifer, A., Brandon, E. P., Kootstra, N., Gage, F. H., and Verma, I. M. Delivery of the Cre recombinase by a self-deleting lentiviral vector: efficient gene targeting in vivo. Proc Natl Acad Sci U S A, *98:* 11450-11455, 2001.
32. Barclay, W. W., Woodruff, R. D., Hall, M. C., and Cramer, S. D. A system for studying epithelial-stromal interactions reveals distinct inductive abilities of stromal cells from benign prostatic hyperplasia and prostate cancer. Endocrinology, *146:* 13-18, 2005.
33. Deng, Z., Wan, M., and Sui, G. PIASy-mediated sumoylation of Yin Yang 1 depends on their interaction but not the RING finger. Mol Cell Biol, *27:* 3780-3792, 2007.
34. Dimri, G. P., Lee, X., Basile, G., Acosta, M., Scott, G., Roskelley, C., Medrano, E. E., Linskens, M., Rubelj, I., Pereira-Smith, O., and et al. A biomarker that identifies senescent human cells in culture and in aging skin in vivo. Proc Natl Acad Sci U S A, *92:* 9363-9367, 1995.
35. Vlahos, C. J., Matter, W. F., Hui, K. Y., and Brown, R. F. A specific inhibitor of phosphatidylinositol 3-kinase, 2-(4-morpholinyl)-8-phenyl-4H-1-benzopyran-4-one (LY294002). J Biol Chem, *269:* 5241-5248, 1994.
36. Chou, T. C. and Talalay, P. Quantitative analysis of dose-effect relationships: the combined effects of multiple drugs or enzyme inhibitors. Adv Enzyme Regul, *22:* 27-55, 1984.
37. Zhuang, S. H., Schwartz, G. G., Cameron, D., and Burnstein, K. L. Vitamin D receptor content and transcriptional activity do not fully predict antiproliferative effects of vitamin D in human prostate cancer cell lines. Mol Cell Endocrinol, *126:* 83-90, 1997.
38. Ihle, N. T. and Powis, G. Take your PIK: phosphatidylinositol 3-kinase inhibitors race through the clinic and toward cancer therapy. Mol Cancer Ther, *8:* 1-9, 2009.
39. Berquin, I. M., Min, Y., Wu, R., Wu, J., Perry, D., Cline, J. M., Thomas, M. J., Thornburg, T., Kulik, G., Smith, A., Edwards, I. J., D'Agostino, R., Zhang, H., Wu, H., Kang, J. X., and Chen, Y. Q. Modulation of prostate cancer genetic risk by omega-3 and omega-6 fatty acids. J Clin Invest, *117:* 1866-1875, 2007.
40. Nelson, E. C., Evans, C. P., Mack, P. C., Devere-White, R. W., and Lara, P. N., Jr. Inhibition of Akt pathways in the treatment of prostate cancer. Prostate Cancer Prostatic Dis, *10:* 331-339, 2007.
41. Beer, T. M., Eilers, K. M., Garzotto, M., Egorin, M. J., Lowe, B. A., and Henner, W. D. Weekly high-dose calcitriol and docetaxel in metastatic androgen-independent prostate cancer. J Clin Oncol, *21:* 123-128, 2003.

42. Beer, T. M. and Myrthue, A. Calcitriol in the treatment of prostate cancer. Anticancer Res, *26:* 2647-2651, 2006.
43. Beer, T. M., Ryan, C. W., Venner, P. M., Petrylak, D. P., Chatta, G. S., Ruether, J. D., Redfern, C. H., Fehrenbacher, L., Saleh, M. N., Waterhouse, D. M., Carducci, M. A., Vicario, D., Dreicer, R., Higano, C. S., Ahmann, F. R., Chi, K. N., Henner, W. D., Arroyo, A., and Clow, F. W. Double-blinded randomized study of high-dose calcitriol plus docetaxel compared with placebo plus docetaxel in androgen-independent prostate cancer: a report from the ASCENT Investigators. J Clin Oncol, *25:* 669-674, 2007.
44. Majumder, P. K., Grisanzio, C., O'Connell, F., Barry, M., Brito, J. M., Xu, Q., Guney, I., Berger, R., Herman, P., Bikoff, R., Fedele, G., Baek, W. K., Wang, S., Ellwood-Yen, K., Wu, H., Sawyers, C. L., Signoretti, S., Hahn, W. C., Loda, M., and Sellers, W. R. A prostatic intraepithelial neoplasia-dependent p27 Kip1 checkpoint induces senescence and inhibits cell proliferation and cancer progression. Cancer Cell, *14:* 146-155, 2008.
45. Yang, E. S. and Burnstein, K. L. Vitamin D inhibits G1 to S progression in LNCaP prostate cancer cells through p27Kip1 stabilization and Cdk2 mislocalization to the cytoplasm. J Biol Chem, *278:* 46862-46868, 2003.

Supplemental Table 1) Syergism between 1,25(OH)2D3 and API-2***

	$1,25(OH)_2D_3$, nM	API-2, μM	CI*	DRI**		Synergism
				$1,25(OH)_2D_3$	API-2	
WFU273CA						
	1	0.1	0.442	11.1	2.8	Intermediate
	10	0.025	0.705	1.6	14.2	Intermediate
	10	0.05	0.324	4.1	12.8	Intermediate
	10	0.1	0.134	15.3	14.6	Strong

*Combination Index (CI<0.1 indicates Very Strong Synergism; 0.1÷0.3 Strong Synergism; 0.3÷0.7 Synergism; 0.70÷0.85 Moderate Synergism; 0.85÷0.90 Slight Synergism; 0.90÷1.10 Nearly Additive Synergism)
**Dose Response Index
*** Data are from assays depicted in Figure S3A, only statistically significantly different means by ANOVA are depicted.

Supplemental Table 2 Induction of senescence in WFU273Ca primary prostate cancer cells*

1,25D3 / API-2	Vehicle	0.1nM	1nM	10nM	100nM
Vehicle	1.8(±0.4)[a]	2.8(±0.6)[a]	4.9(±2.8)[a]	7.3(±1.3)[a]	16.8(±2.3)[b]
0.01 µM	5.9(±1.1)[a]	3.5(±0.9)[a]			
0.05 µM	2.8(±0.5)[a]		3.8(±0.7)[a]		
0.1 µM	6.5(±1.2)[a]			24.0 (±5.6)[c]	
0.5 µM	30.0(±3.0)[b]				

*Percent of senescent cells as determined by (SA)-β-galactosidase activity. Means ± SE are shown. Means without a common letter are significantly different by ANOVA, $p < 0.05$.

Supplemental Figure 1

A

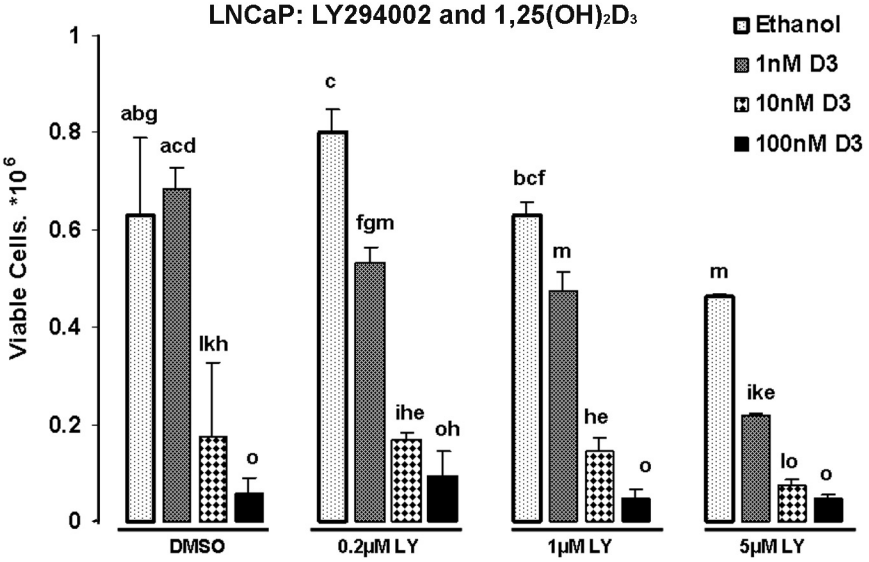

B

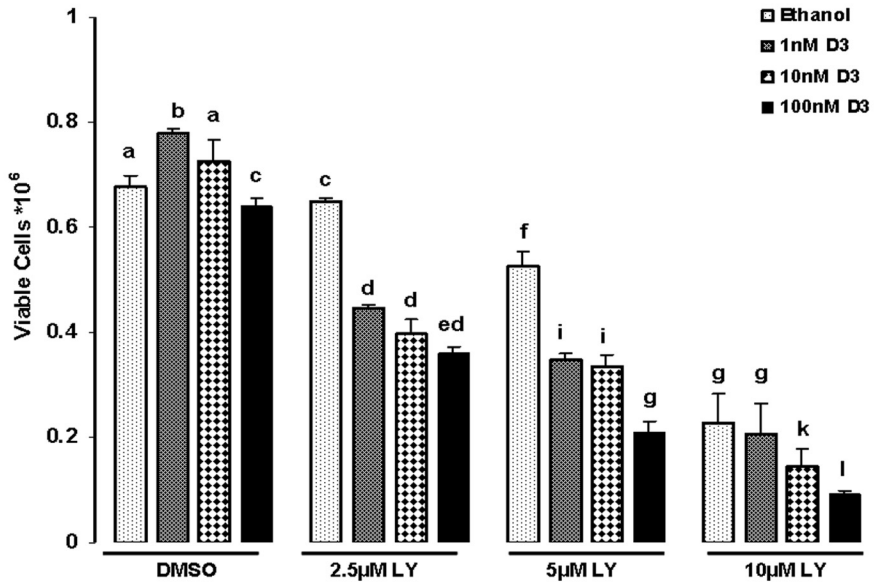

C

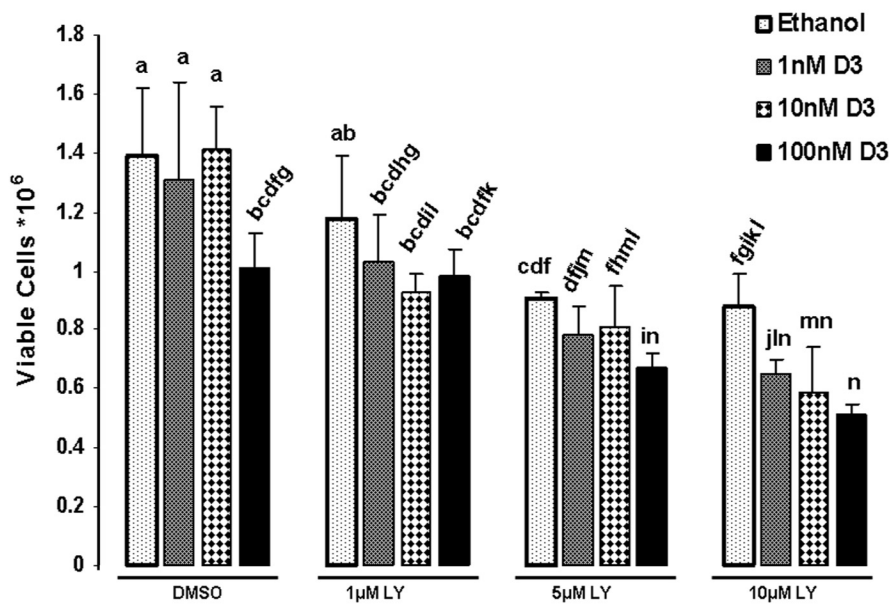

Supplemental Figure 2

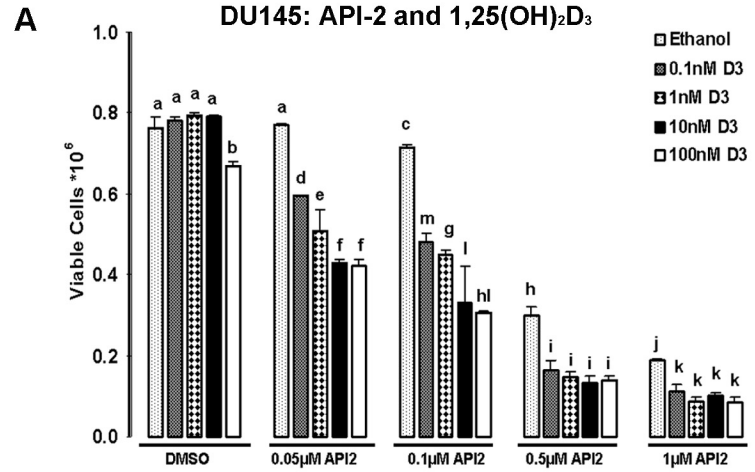

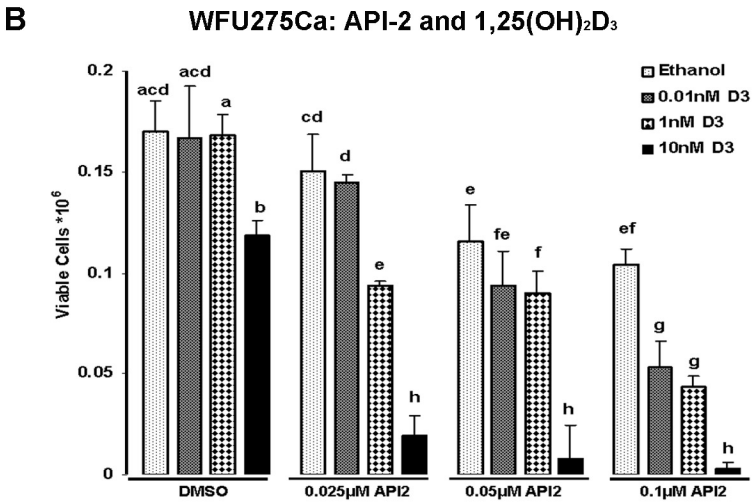

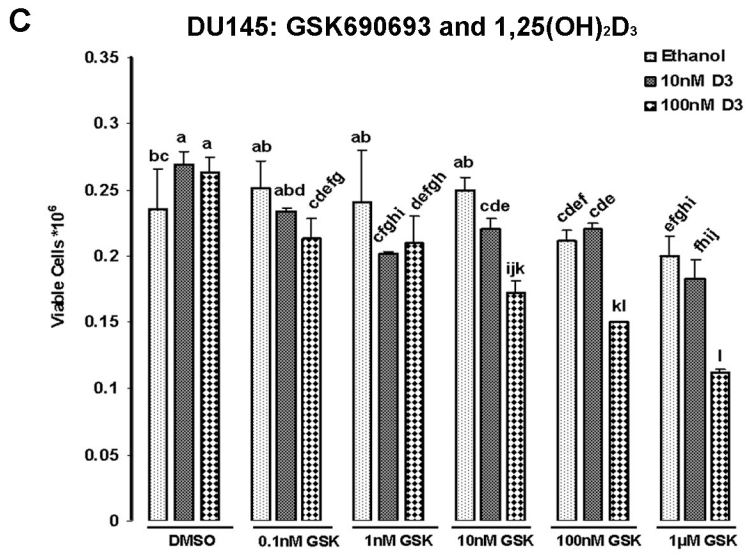

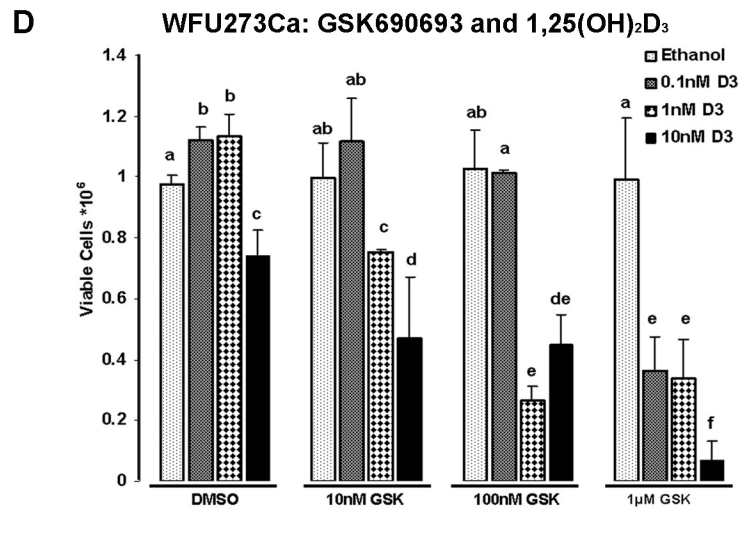

Supplemental Figure 3

A

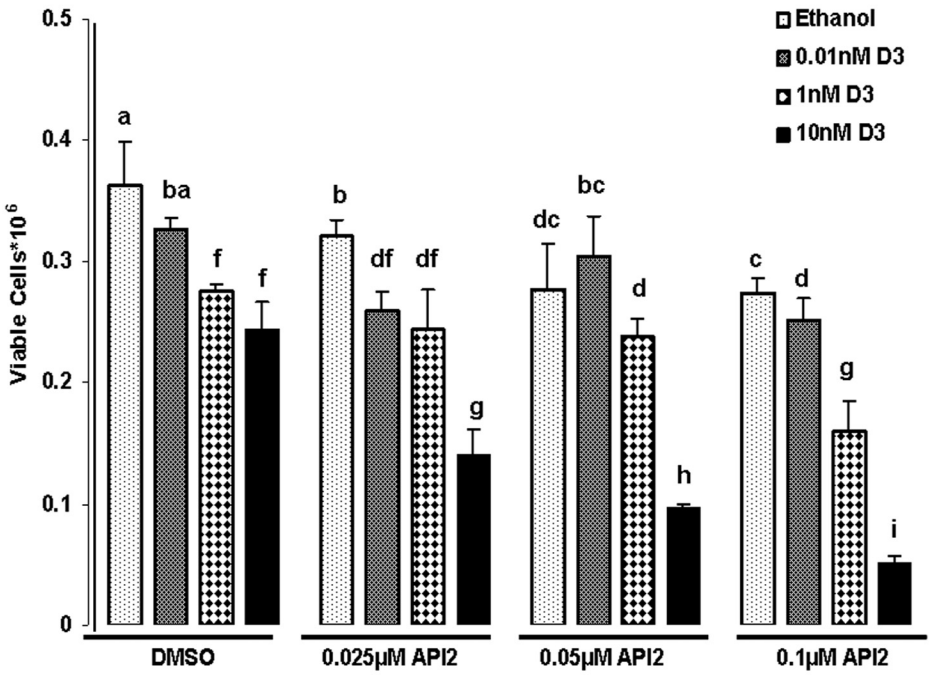

B

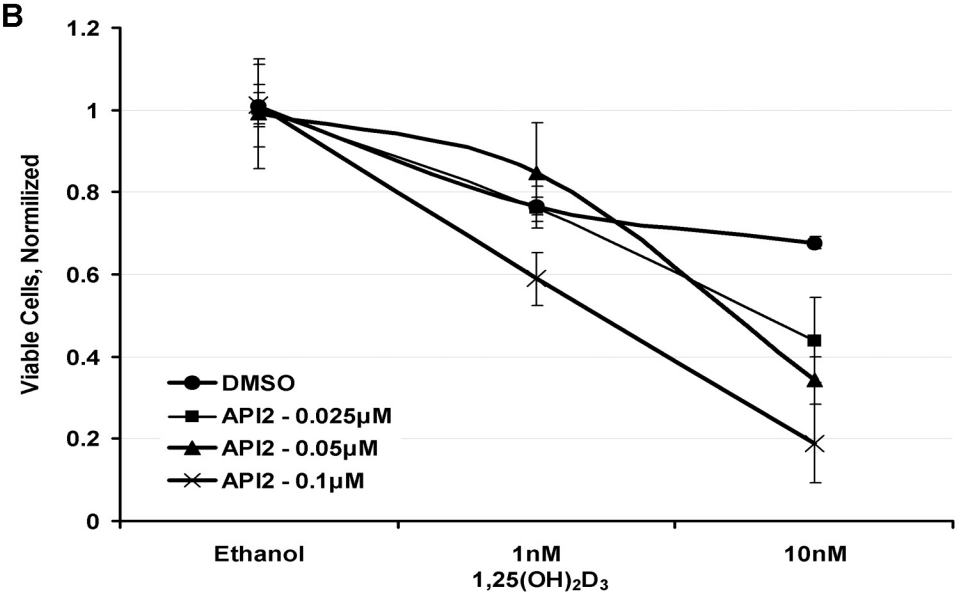

Supplemental Figure 4

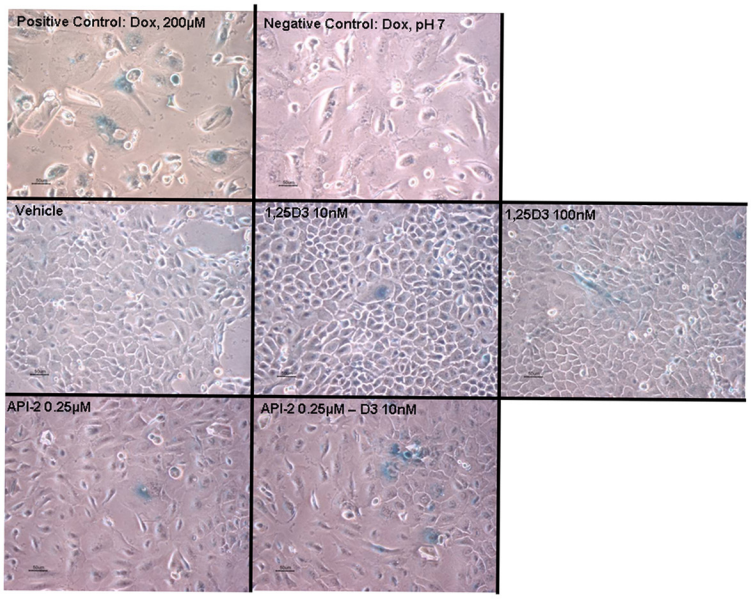

Supplemental Figure 5

A

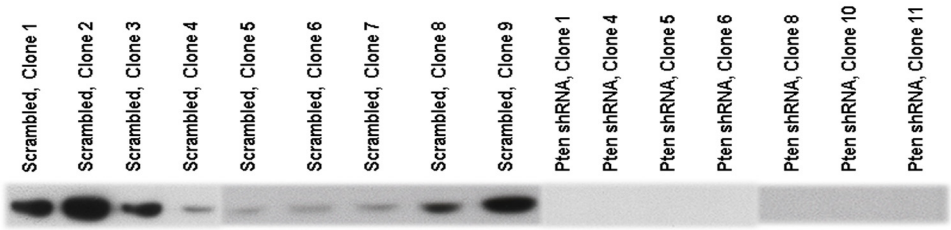

B

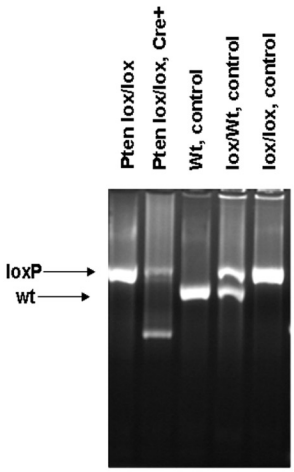

C

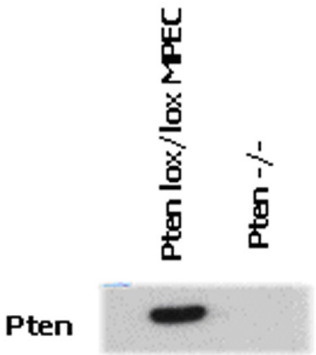

Supplemental Figure 6

A

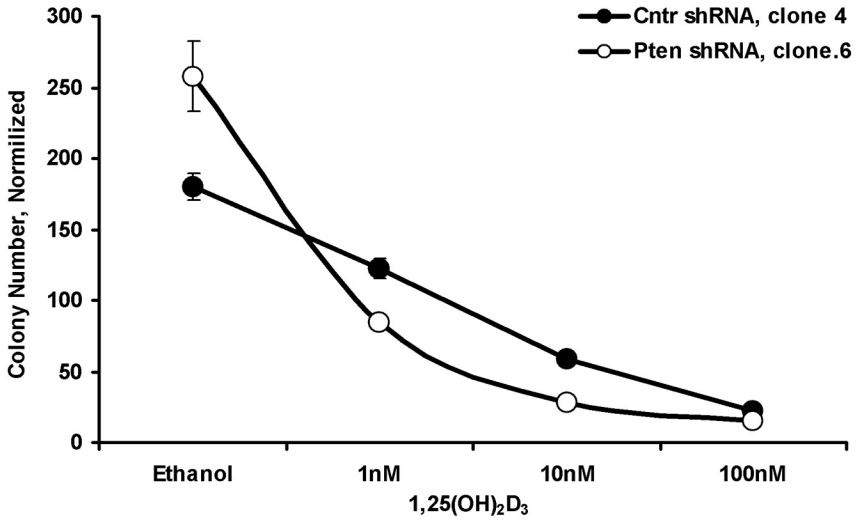

B

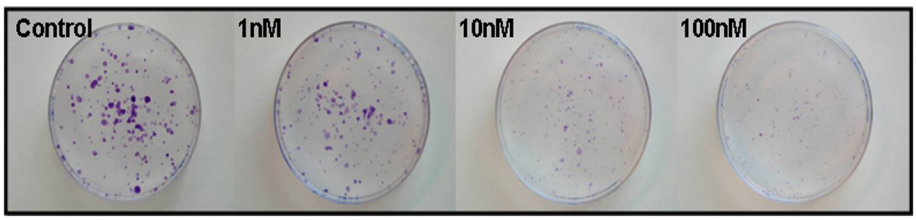

C

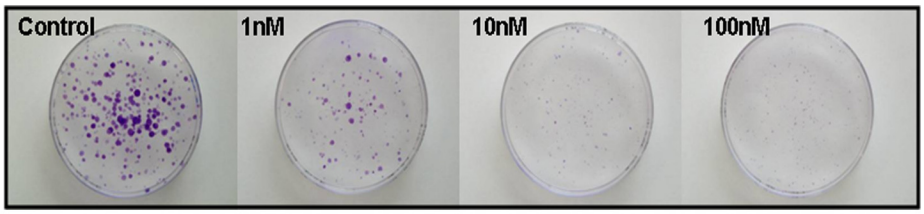

Supplemental Figure 7

A

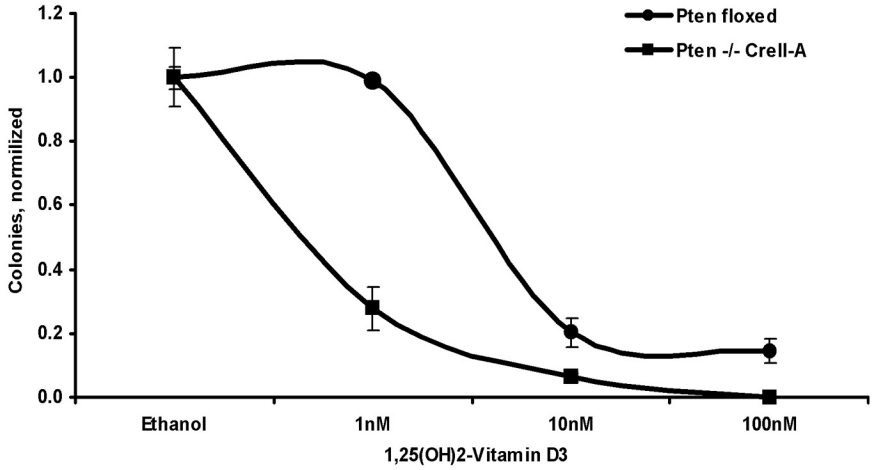

B

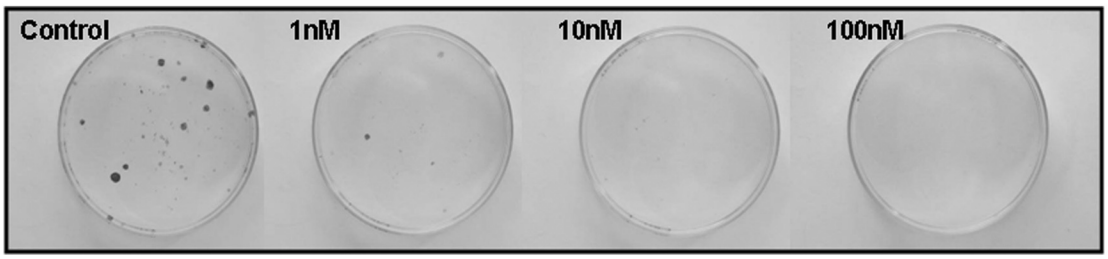

C

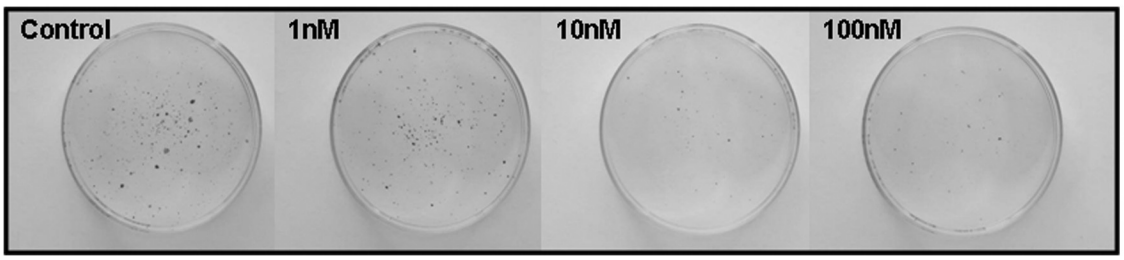

Supplemental Information.

Materials and Methods:

Real-time PCR for evaluation of Pten deletion. Genomic DNA was extracted from MPEC and real-time PCR was performed for Pten lacking exon 5, Pten WT and Pten Lox site using iCycler (Bio-Rad) with QuantiTect SYBR Green PCR kit (QIAGEN) as previously described(24). PCR reaction consisted of 50 cycles of 15 seconds at 94°C, 30 seconds at 57°C, and 45 seconds at 72°C. Reaction mixtures without genomic DNA were used as negative controls.

Immunoblot:. Plates were washed twice with cold PBS, lysis buffer (5mM EDTA, 150mM NaCl, 50mM Tris-HCl, 1% NP-40) containing freshly added protease inhibitor cocktail (PIC), 1mM DTT, 1mM Na3VO4 and 5mM NaF was added to the plates. Plates were placed on ice for 20min with tilting every 5min. Cells were scrapped and collected into eppendorf tubes, centrifuged at 13000rpm for 15min at 4ºC. Supernatants were collected and stored at -80ºC. 50-100µg of protein was subjected to electrophoresis on SDS-PAGE gels. Proteins were transferred onto prewetted Hybond-P PVDF (polyvinylidene diflouride) membrane according to manufactures' protocol (Amersham Pharmacia Biotech, Buckinghamshire, UK). Membranes were incubated with appropriate dilutions of Pten (sc-7974) (Santa Cruz Biotechnology, Santa Cruz, CA). Secondary antibodies conjugated to horse radish peroxidase (Santa Cruz Biotechnology) were used. ECL Plus Western Blotting Detection System kit (Amersham-Pharmacia) was used for detection of proteins.

Clonogenic survival assays. Cells were plated in 6-cm diameter dishes at 2000 or 4000 cells per plate in medium containing 1nM, 10nM or 100nM $1,25(OH)_2D_3$ or vehicle (ethanol, 1x = 0.1% V/V) and allowed to grow for 7 days. Platings were performed in quadruplicate. After incubation, cells were fixed with 10% methanol–10% acetic acid and stained with a 0.4% solution of crystal violet. Colonies with >50 cells were counted. Error bars represent SD.

Supplemental Figure Legends:

Supplemental Figure 1. LY294002 synergizes with 1,25(OH)$_2$D$_3$ to inhibit growth of LNCaP, DU145 cells and Pten-/- MPEC.

Growth inhibition of LNCaP cells **(A)**, DU145 cells **(B)** and Pten$^{-/-}$ MPEC (clone 11) **(C)** treated with 1,25(OH)$_2$D$_3$ in presence or absence of LY294002. Cells were grown and treated as described in Materials and Methods. Viable cells were counted with a hemacytometer after trypan blue exclusion and presented as means for the triplicates +SD. Means without a common letter are significantly different by ANOVA ($P < 0.05$).

Supplemental Figure 2. Inhibition of AKT with API-2 or GSK690693 synergizes with 1,25(OH)$_2$D$_3$ to inhibit growth of prostate cancer cells.

(A) Growth inhibition of DU145 cells treated with 1,25(OH)$_2$D$_3$ in presence or absence of API-2. **(B)** Growth inhibition of WFU275Ca cells treated with 1,25(OH)$_2$D$_3$ in presence or absence of API-2. **(C)** Growth inhibition of DU145 cells treated with 1,25(OH)$_2$D$_3$ in presence or absence of GSK690693. **(D)** Growth inhibition of WFU273Ca cells treated with 1,25(OH)$_2$D$_3$ in presence or absence of GSK690693. Cells were grown and treated as described in Materials and Methods. Viable cells were counted with a hemacytometer after trypan blue exclusion and presented as means for the triplicates +SD. Means without a common letter are significantly different by ANOVA ($P < 0.05$).

Supplemental Figure 3. API-2 synergizes with 1,25(OH)$_2$D$_3$ to inhibit growth of human primary prostate cancer cell strain WFU273Ca.

(A) Growth inhibition of WFU273Ca cells in response to API-2 and 1,25(OH)$_2$D$_3$ alone or in combination. Cells were grown treated as described in Materials and Methods. Viable cells were counted with a hemacytometer after trypan blue exclusion and presented as means for the triplicates +SD. Means without a common letter are significantly different by ANOVA ($P < 0.05$). **(B)** Number of viable cells normalized to control presented as means ± SD.

Supplemental Figure 4. 1,25(OH)$_2$D$_3$ and API-2 induce senescence in cooperative manner in DU145 cells. Cells were grown, treated and (SA)-β-galactosidase activity was evaluated as described in Materials and Methods. Representative photographs taken at 20X magnification are demonstrated**.**

Supplemental Figure 5.

(A) Immunoblot analysis of Pten expression in WFU3 MPEC infected with Pten shRNA or scrambled shRNA as described in Materials and Methods.

(B) PCR analysis of Pten deletion by self-deleting Cre-recombinase lentivirus in Pten$^{lox/lox}$ MPEC. Pten$^{lox/lox}$ MPEC isolated from 8 weeks old Pten lox/lox Cre-recombinase negative animals and infected with self-deleting Cre-recombinase lentivirus to generate Pten$^{-/-}$ MPEC.

(C) Immunoblot analysis of Pten deletion by self-deleting Cre-recombinase lentivirus in $Pten^{lox/lox}$ MPEC. $Pten^{lox/lox}$ MPEC isolated from 8 weeks old $Pten^{lox/lox}$ Cre-recombinase negative animals and infected with self-deleting Cre-recombinase lentivirus.

Supplemental Figure 6. *In vitro* suppression of Pten with shRNA doesn't affect clonogenic survival of cells in response to $1,25(OH)_2D_3$. Clonogenic surival**(A)** and representative photographs of clonogenic survival of WFU3 MPEC (Pten shRNA, clone 6) **(B)** and WFU3 MPEC scrambled shRNA (clone 4)**(B)** treated with increasing concentrations of $1,25(OH)_2D_3$. Cells were plated at 2000 cells per 60mm tissue culture dish. Values are average for quadruplicates±SD are demonstrated.

Supplemental figure 7. *In vitro* loss of Pten doesn't affect clonogenic survival of cells in response to $1,25(OH)_2D_3$. Clonogenic surival **(A)** and representative photographs of clonogenic survival of $Pten^{lox/lox}$ MPEC **(B)** and respective $Pten^{-/-}$ MPEC ($Pten^{lox/lox}$ MPEC infected with self-deleting Cre-recombinase) **(C)** treated with increasing concentration of $1,25(OH)_2D_3$. Pten lox/lox MPEC were plated at 2000 cells per 60mm tissue culture dish and at 4000 cells per dish for $Pten^{-/-}$ MPEC. Values are average for quadruplicates±SD.